2008

ASSESSMENT AND POTENTIAL ADJUSTMENTS TO THE SNOW-RELATED ALGORITHMS IN BIOME-BGC, v4.2

Deana Ann DeWire
The University of Montana

ASSESSMENT AND POTENTIAL ADJUSTMENTS

TO THE SNOW-RELATED ALGORITHMS IN BIOME-BGC, v4.2

By

Deana Ann DeWire

B.A., Kutztown University, Kutztown, Pennsylvania, 2001

Thesis

Presented in partial fulfillment of the requirements
for the degree of

Master of Arts
in Geography

The University of Montana
Missoula, MT

Autumn 2008

Approved by:

Perry Brown, Associate Provost
Graduate Education

Dr. Anna E. Klene, Chair
Geography

Dr. Ulrich Kamp,
Geography

Dr. Joel T. Harper,
Geosciences

Dr. Faith Ann Heinsch,
Forestry

DeWire, Deana, M.A., Autumn 2008 Geography

Assessment and Potential Adjustments to the Snow-Related Algorithms in BIOME-BGC, v.4.2

Chairperson: Anna E. Klene

Many watersheds throughout the mountain west are snow-melt dominated. Recent studies suggest that climatic shifts throughout the 20th century have diminished snowpack around the west, a trend that may accelerate in the future. Loss of critical snowpack could negatively affect the ecosystems and communities that have come to depend on it. Process models offer a way to illuminate the effects of climate change on snowpack. BIOME-BGC, a well established eco-system process model, contains a simple snow melt model for predicting daily snow water equivalent (SWE). The model requires standard daily meteorological data and can, therefore, be extrapolated over long periods of record. This research evaluated the effectiveness of BIOME-BGC (v4.2) at predicting SWE, snowpack evolution, and soil temperature. Then, several physically based algorithms were incorporated into current model logic and model behavior was evaluated. Finally, a new degree-day algorithm was presented and assessed for inclusion into future versions of BIOME-BGC. The study concluded that the new degree-day algorithm should be investigated further as it offered the best results.

Acknowledgements

I have drawn on the individual expertise of each member of my committee. Without each of them I would have been at a great loss in this work. They have been very patient and understanding with me throughout this process, and for this I am truly grateful. Dr. John Kimball has also been exceptionally helpful and his guidance helped me obtain the theoretical background necessary to complete this work.

The love and encouragement of my family has helped me maintain perspective while completing my graduate work. Even though they were thousands of miles away, the knowledge that we live in each others hearts and minds kept me going when things felt overwhelming.

The support of my friends and fellow graduate students is unmatched; especially my best friend, who has been my rock and guiding light through most of this process. He has held my hand, fed me well and wiped away my tears. There are not words to describe how thankful I am. Now we move into the unknown.

Table of Contents

LIST OF FIGURES

LIST OF TABLES

Chapter 1: Introduction

The interaction between mountainous terrain and climate, although well studied, is complex and highly variable. Mountains tend to create their own weather patterns and can dramatically modify synoptic weather systems (Barry, 1981). It is universally accepted that orographic uplift results in increased precipitation. However, elevation alone is a poor determinant of increased precipitation. An increase in mountain precipitation occurs because of the interaction among several topographic factors, including orientation, relief, elevation, and exposure (Spreen, 1947).

During the winter months, most high-elevation precipitation falls as snow. Snowpack accounts for 50% to 70% of mountain precipitation in the western United States (Serreze et al., 1999) and is of immense importance to western communities that depend on it for their drinking water, irrigation, power, and recreation-based economies. In western Montana, 62% of annual precipitation is snowfall (Serreze et al., 1999). The accumulation of snow through the winter stores water that is released during the spring and summer thaw. This is why mountains are often called the world's "water towers"; between 60% and 80% of moving freshwater originates there (Viviroli et al., 2003).

Orographic uplift is an important contributor to mountain snowpack, however, it is only capable of producing the same amount of precipitation that would result from a convective or cyclonic disturbance in the absence of a topographic barrier (Barry, 1981). Global and regional climate patterns and disturbances that affect atmospheric moisture are, therefore, critical influences on the development of seasonal mountain snowpack.

There is evidence that snow resources throughout western North America have diminished since the middle of the 20th century (Hamlet, Mote, Clark, & Lettenmaier,

2005; Mote, 2006; Mote et al., 2005). Some research (Barnett et al., 2008) suggests that warming temperatures are largely responsible for the changes in snow hydrology throughout the West, while others (Moore et al., 2007) propose that precipitation is more influential. Recent research also suggests there is an inverse relationship between Northern Rockies snowpack and Pacific Ocean oscillations (Cayan et al., 1999; Kunkel & Angel, 1999; McCabe & Dettinger, 2002; Selkowitz et al., 2002; Smith & O'Brien, 2000). Declining snowpack due to anthropogenic climate change (Barnett et al., 2008; Cooley, 1990) and natural variability may affect stream flow amount and timing throughout the west (Barnett et al., 2008; Cooley, 1990; Regonda et al., 2005; Stewart et al., 2005) . The presence of snow can also affect soil temperatures, which, in turn, influence run-off, soil genesis and soil respiration (Bayard et al., 2005; Lagergren et al., 2006; Retzer, 1974; Shanley & Chalmers, 1999).

Continuous snowpack monitoring is done at SNOTEL locations throughout the western United States; however, this data is sparse in both temporal and geographic extent. Process models are useful for assessing snowpack variability at locations where no monitoring is done and for time periods devoid of data. Hydro-ecologic modeling of future climate change scenarios generally predict further reduction in snowpack development and an advancement in snowmelt runoff (Lapp, et al., 2005; Mote et al., 2003; Payne et al., 2004).

1.1 Objectives

This research explored the ability of a highly simplified snow model to predict snowpack development and evolution and soil temperature at point locations in the

Rattlesnake Creek watershed, north of Missoula, Montana. BIOME-BGC, an eco-physiological process model, contains a very simple snowpack and soil temperature sub-routine. The first phase of this research assessed snow and soil-temperature related output from BIOME-BGC, v4.2; a process model that could be used to examine snowpack response to climate perturbations.

The second objective of this research was to evaluate several potential algorithm modifications for increased accuracy. Current BIOME-BGC logic sacrifices fundamental physics related to snow in exchange for model simplicity. This study investigated how including basic snow processes affected model performance. Algorithms were only considered if they easily fit within the basic framework of the current model. The accuracy of the altered subroutines was assessed to see if it improved upon the performance of BIOME-BGC, v4.2.

1.2 Study Area

The 208 km² Rattlesnake Creek watershed forms the northern edge of Missoula's city limit and extends north into the Rattlesnake Wilderness area (Figure 1.1). The terrain is highly variable, with slopes ranging from 0° along the river valley to 75° at mid-slope locations. The elevation ranges from 975 m ase in the valley to 2630 m ase at McLeod peak.

Rattlesnake Creek is a fourth-order stream according to Horton's morphometric system of stream classification. There are six catchment basins within the larger Rattlesnake Creek drainage. Rattlesnake Creek flows south to its terminus at the confluence with the Clark Fork River.

December is the coldest month of the year in Missoula, with a mean daily max temperature of -1°C and low of -8°C (NCDC, 2002). Conversely, July is the warmest month with mean daily low and high temperatures ranging between 10°C and 28.5°C (NCDC, 2002). Average annual precipitation at the airport is 351 mm, with May receiving the most precipitation (NCDC, 2002). Annual snowfall at the airport is 1112 mm, mostly falling in December and January (NCDC, 2002).

There is a deficiency of climate research for the Rattlesnake Mountains; however, some work has been done in the nearby Bitterroot Mountains. Finklin (1983) discovered that winter winds are generally light, but can be locally extreme on the ridge tops. Precipitation falling as snow increased by 50% at 1525 m and 70% at 2135 m, with snow cover persisting into mid-June. The wettest months in the Bitterroot Mountains are November, December, and January (Finklin, 1984).

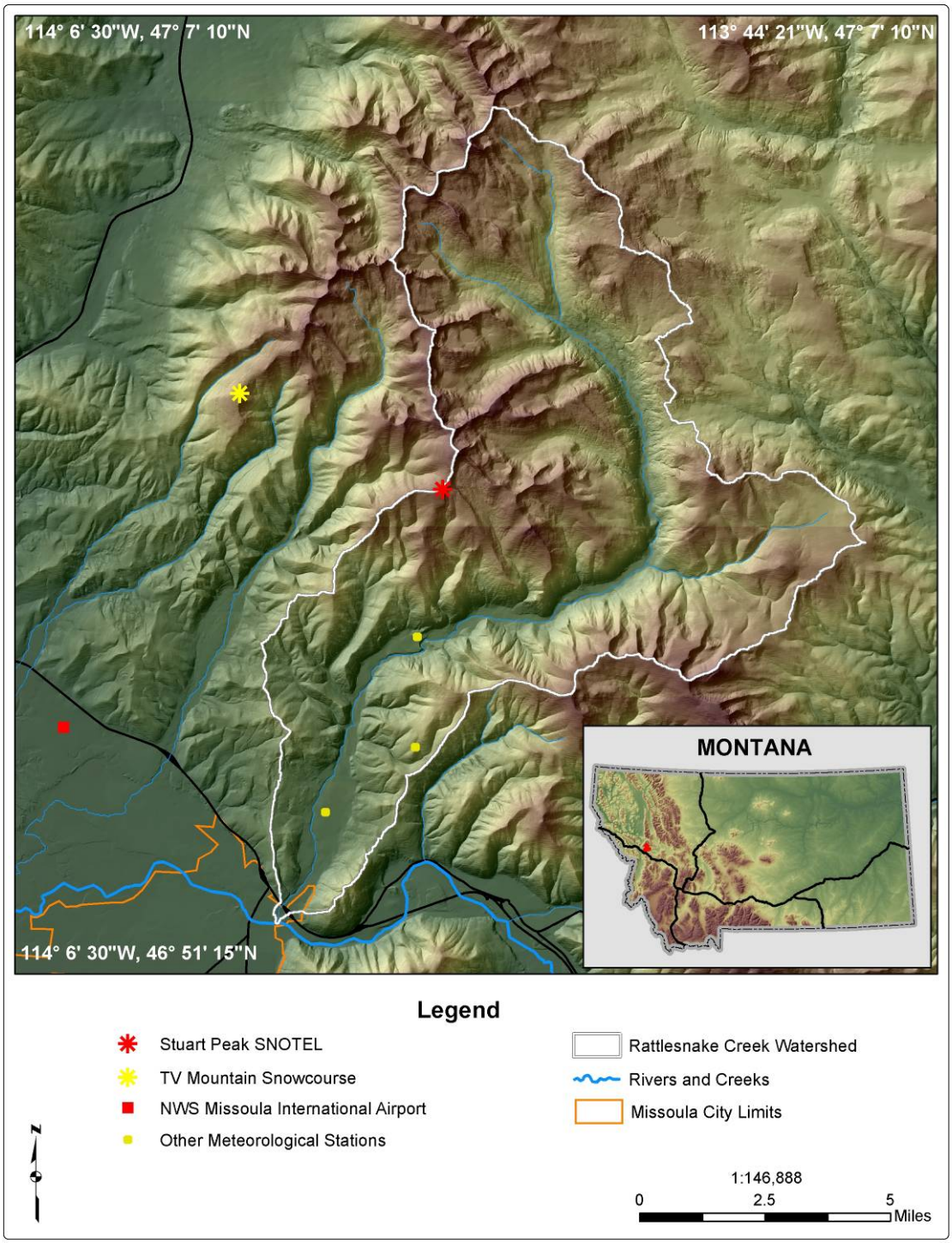

Figure 1.1 Map of the study area showing the Rattlesnake Creek watershed and existing meteorological stations.

Chapter 2: Validation of Selected Variables from BIOME-BGC

2.1 Introduction

This chapter describes the logic of MT-CLIM and BIOME-BGC (v4.2) as it relates to this research. Input and validation data are described. Model output was validated using measured data at sites in and around the Rattlesnake Creek watershed.

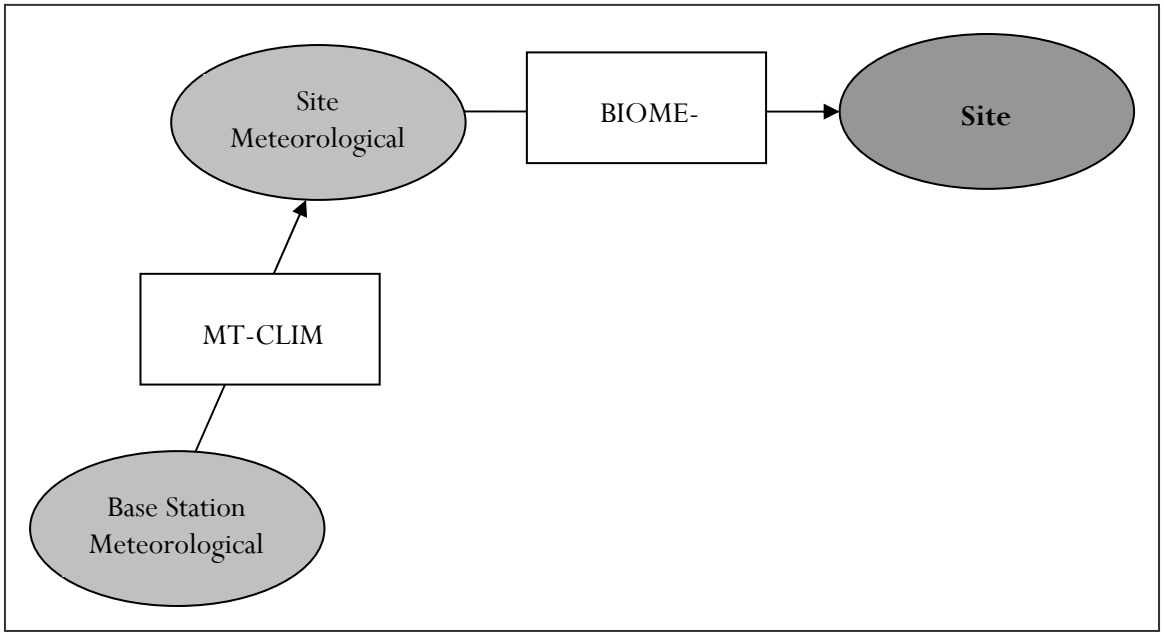

Figure 2.1 Flow chart for modeling ecophysiological processes using MT-CLIM and BIOME-BGC.

2.2 Model Description

2.2.1 MT-CLIM

Due to the geographic paucity of meteorological data in the area, the climate simulation model MT-CLIM, was employed to extrapolate daily meteorological data from a base station to remote study sites. MT-CLIM was specifically designed to provide input for process-based ecophysical models such as BIOME-BGC, DAYTRANS, and

RHESSys (Running et al., 1987). A schematic of model work flow is illustrated in Figure 2.1.

MT-CLIM requires daily meteorological inputs from the base station, as well as a geographical description of the base station and study site. Appendix A provides a full description of MT-CLIM initialization files. The lapse rate for maximum and minimum temperature must also be defined. Meteorological input includes daily maximum and minimum air temperature and total daily precipitation. Daily dew-point temperature is an optional input; minimum daily air temperature is used as a surrogate for dew point when measured data is not available (Running et al., 1987). Missoula International Airport served as the primary base station data for this research.

Calculations for daily minimum and maximum air temperature assume a linear relationship between temperature and elevation. Maximum daily air temperature is calculated based on a user-defined lapse rate:

$$T_{max} = T_{max,base} + ((Elevation_{site} - Elevation_{base}) * LR_{Tmax}), \quad \text{(eq. 2.1)}$$

where $T_{max,base}$ is the maximum daily air temperature recorded at the base station, $Elevation_{site}$ is the elevation of the study site, $Elevation_{base}$ is the elevation at the airport, and LR_{Tmax} is the lapse rate for maximum daily air temperature (°C/km). The default lapse rate for the maximum daily temperature is set to the lapse rate of -6°C/km. Minimum daily temperature lapse rate is set at -3°C/km. Minimum daily air temperature is calculated following the same logic as maximum daily air temperature. Precipitation is calculated following a linear function similar to the calculation for maximum and minimum daily air temperature.

Daily solar radiation calculations are based on the work presented by Briostow & Campbell (1984). Their logic has been extended to produce accurate results in a variety of climates without site specific parameterization (Thorton & Running, 1999). Calculations consider the effects of an obstructed horizon and snowpack on incoming radiation (Thornton et al., 2000). Humidity and radiation are related and predicted jointly (Thornton et al., 2000). Daily surface humidity is adjusted for arid conditions when the ratio between potential evapotraspiration and precipitation is greater than 2.5 (Kimball et al., 1997). For all other sites, daily dew-point temperature is set equal to the daily minimum temperature (Running et al., 1987). Day length, also important to radiation and humidity calculations, is considered the time the sun is above the horizon and is calculated based on the latitude of the site (Hungerford et al., 1989).

2.2.2 BIOME-BGC

BIOME-BGC is a general ecosystem process model that computes forest carbon, water, and nitrogen cycles on a daily time-step (Figure 2.2; Running & Hunt, 1993). Spatially, the model's simplistic one-dimensional structure does not allow for horizontal or lateral energy transfer (Thornton, 1998). Calculations are quantified within a horizontal grid-unit, assumed to be homogeneous, that defines the physical boundaries of the simulation (Thornton, 1998). BIOME-BGC requires daily input for day length, maximum and minimum air temperature, daylight average air temperature, total precipitation, total incident shortwave radiation, and daytime vapor pressure deficit (Appendix B contains the initialization parameters used for BIOME-BGC model runs).

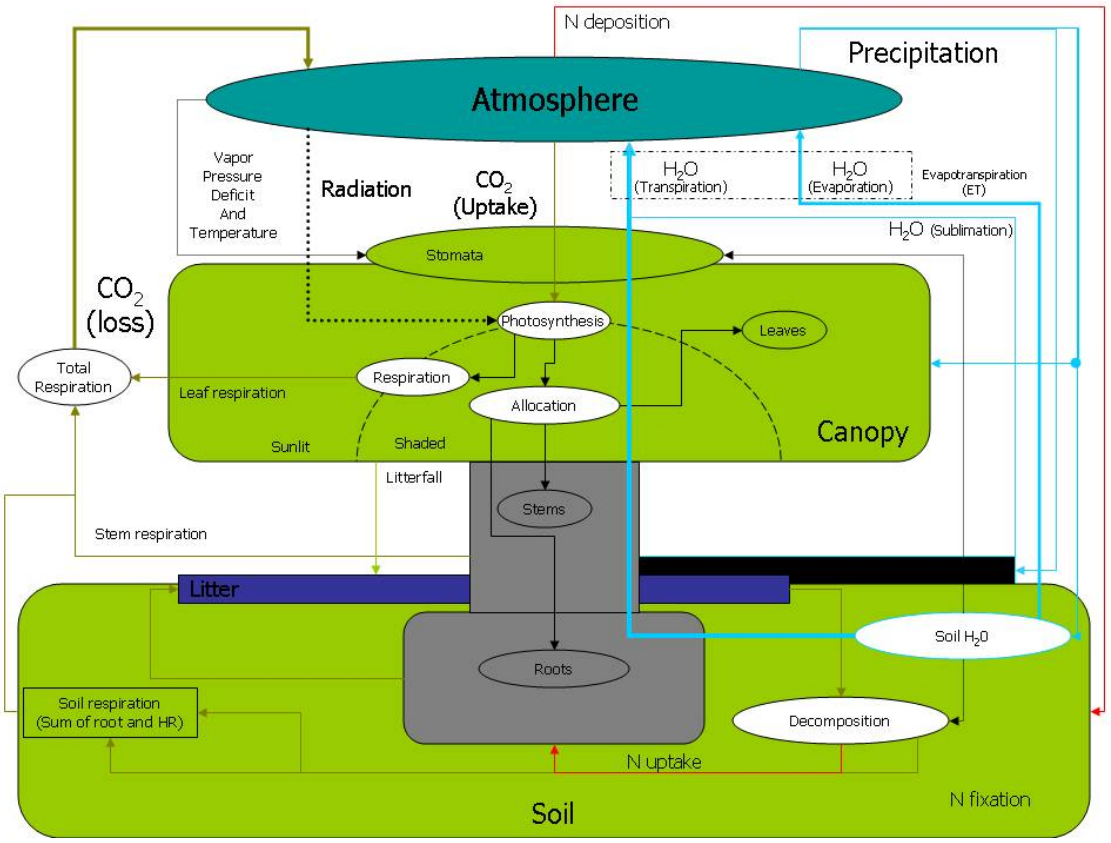

Figure 2.2. Conceptual diagram of the processes recognized by BIOME-BGC, v4.2. Hydrologic processes are illustrated in light blue.

The snow routine of BIOME-BGC has been successfully employed in several studies to assess model accuracy and snowpack sensitivity (Coughlan & Running, 1997; Kimball et al., 1997; Running & Nemani, 1991). BIOME-BGC, v4.2, approaches snowpack in a highly simplified way. Daily precipitation is routed to the snowpack, measured as millimeters of snow-water equivalent (SWE), when the average daily temperature is at or below freezing (Thornton, 1998). The model does not recognize canopy interception of snow (Thornton, 1998).

Ablation occurs within BIOME-BGC through sublimation and melting. Snowpack is lost to sublimation (R_{sub}) only when the mean daily temperature is below freezing and is calculated by:

$$R_{sub} = R / LH_{sub}, \quad \text{(eq. 2.2)}$$

where R is the incident radiation and LH_{sub} is the latent heat of sublimation (2845 kJ/kg) (Coughlan, 1991). Snowmelt is driven by both temperature and radiation. Temperature-driven snowmelt (T_{melt}) is estimated by:

$$T_{melt} = t_{coef} * T_{avg} \text{ when } T_{day} >= 0°C, \quad \text{(eq. 2.3)}$$

where t_{coef} is a snowmelt coefficient equal to 0.65 kg $H_2O/m^2/d/°C$ and T_{avg} is the mean daily temperature. Daily snowmelt due to radiation (R_{melt}) is calculated as:

$$R_{melt} = R / LH_{fus} \text{ when } T_{day} >= 0°C, \quad \text{(eq. 2.4)}$$

where LH_{fus} is the latent heat of fusion (335 kJ/kg). A logic test is performed on total daily snowmelt, the sum of R_{melt} and $T_{melt,}$, to ensure that it is not greater than the accumulated snowpack. Daily melt enters the soil water compartment or runs off (Thornton, 1998).

Soil temperature under a snowpack is estimated in BIOME-BGC as a weighted 11-day running average, such that

$$T_{soil} = T_{ra} + 0.83(T_y - T_{ra}) \quad \text{(eq. 2.5)}$$

where T_{soil} is the soil temperature in the upper 10 cm of the soil, T_{ra} is the 11-day running average and T_y is the annual air temperature (Zheng et al., 1993).

2.3 Methods

2.3.1 Input and Validation Data

Four meteorological stations were operating in the study area over the 2006-07 winter season. These included a SNOwpack TELemetry (SNOTEL) site, a Cooperative Observer Program (COOP) station, and two weather stations deployed by the University of Montana, Department of Geography (Figure 1.1). The Department of Geography chose station installation locations to fill mid-elevation data gaps. Both stations were installed in open canopy sites (Figure 2.3). Table 2.1 describes the meteorological stations that were used for model input and validation.

Figure 2.3. Picture of one of the weather stations installed by the Department of Geography in the Rattlesnake Creek watershed.

SNOTEL instruments use a solution filled snow pillow and transducer to estimate SWE from the pressure of the overlying snow (Figure 2.4). SNOTEL instrumentation is installed and maintained by the Natural Resource Conservation Service. Error can be introduced into SNOTEL measurements when snow bridging occurs above the snow pillow and when foreign material, such as branches, is deposited on the overlying snowpack (Selkowitz et al., 2002).

Figure 2.4. Picture of the Stuart Peak SNOTEL station.

National Weather Service data collected at the Missoula International Airport provided the "base" station data for MT-CLIM. Missing values in the NWS dataset were replaced with elevationally adjusted COOP station data. Gaps in NWS values that exist prior to the establishment of the COOP station were filled using a linear interpolation of the preceding and following days.

Meteorological Stations In and Adjacent to Study Area																	
Name	**Type**	**Variables Measured**														**Obs. Interval**	**Dates**
		T_{avg}	T_{max}	T_{min}	ST	SWE	SD	SF	P	RH	DP	WD	WS	SR	SP		
Stuart Mountain	**SNOTEL**	x	x	x		x	x	x	x							**3 Hrs**	**1994 – present**
Missoula 2NE	**COOP**	x	x	x					x							**24 Hrs**	**Oct 1966 – present**
Rattlesnake Moraine	**University of MT**	x			x					x		x	x			**1 Hr**	**Nov 2006 – present**
Woods Gulch	**University of MT**	x			x					x		x	x			**1 Hr**	**Nov 2006 – present**
Missoula Airport	**NWS**	x	x	x		x	x	x	x	x	x	x	x	x	x	**1 Hr**	**1935 – present**

Table 2.1 Meteorological stations in or near the Rattlesnake Creek Watershed that were used for model input and validation. Variables are defined as follows: T_{avg} is average temperature, T_{max} is maximum temperature, T_{min} is minimum temperature, ST is soil temperature, SWE is snow water equivalent, SD is snow depth, SF is snowfall, P is precipitation, RH is relative humidity, DP is dew point, WD is wind direction, WS is wind speed, SR is solar radiation, and SP is station pressure.

Systematic precipitation measurement errors, attributable to wind, wetting loss, and evaporation loss, are well documented (Fuchs et al., 2001; Goodison et al., 1981; Groisman et al., 1999; Yang et al., 1998). Daily precipitation recorded at the Airport was corrected for wetting loss and wind-induced under-catch following the methods of Yang et al. (1998).

2.3.2 Model Evaluation

In situ measurements were used to validate BIOME-BGC using a suite of model validation statistics. Validation data consists of daily temperature (T_{min} and T_{max}) and SWE measurements taken in or adjacent to the Rattlesnake Creek watershed. Temperature was validated against daily observations recorded at the sites described in Table 2.1. While a continuous series of daily SWE measurements are available from the

Stuart Peak SNOTEL beginning in 1994, temporally discrete SWE measurements are available from the Natural Resource Conservation Service (NRCS) snow course program at Stuart Peak and T.V. Mountain since 1937 and 1956, respectively.

Rain gauge measurements were not used to assess modeled precipitation. Daily precipitation observations often suffer from systematic measuring errors (Groisman et al., 1999; Groisman & Easterling, 1994; Yang et al., 1998), and should have a gauge-specific correction algorithm applied to the data before being used for model calibration or verification (Fuchs et al., 2000). The validation sites have no wind speed measurements available, so cannot be calibrated in the same way that the Airport data were.

Snowpack evolution characteristics evaluated included snow days, date of snowpack onset, and the date of melt. Snow days consisted of a simple count of days that snow was present throughout a snow year, defined here as beginning on September 1. Snowpack onset and melt attempted to focus on the primary snowpack, which can be nebulous and vary by location. High-elevation sites, such as Stuart Peak, tend to have a persistent snow cover with an easily defined beginning and melt date. Low-elevation sites, on the other hand, can accumulate and melt a snowpack several times throughout the winter. This study used separate methods to evaluate onset and melt dates for low and high elevation sites. The primary snowpack at Stuart Peak was considered underway when 10 continuous days of snow were recorded. The snowpack was assumed to be melted when 10 consecutive snow-free days were recorded. A different method was used at the low-elevation COOP station to define onset and melt dates because there was rarely a clearly definable primary snowpack. Onset was considered the first day that snow was present; melt date was the last day that snow was present. The percentage of snow days

between the onset and melt date was utilized as surrogate measure of primary snowpack at the COOP station.

Snowpack insulates the underlying soil, resulting in soil temperature stabilization (Gustafsson et al., 2001). This allows daily soil temperature flux to be used as a surrogate for the presence or absence of snow. This study assumed that snow was present when the diurnal soil temperature range, measured at the Rattlesnake Moraine and Woods Gulch weather stations, was less than 0.5°C.

Model performance in the Rattlesnake Creek watershed was evaluated against measured air and soil temperature, snow water equivalent (SWE), and snowpack evolution, and using several model validation statistics. Pearson's correlation analysis (r, eq. 2.6), mean absolute error (MAE, eq. 2.7), root mean square error (RMSE, eq. 2.8), the index of agreement (*d,* eq. 2.9), and the Relative Error (RE, %, eq. 2.10) are defined as:

$$r = \frac{[\sum_{i=1}^{N}(P_i - \overline{P})(O_i - \overline{O})]^2}{\sqrt{[\sum_{i=1}^{N}(P_i - \overline{P})^2 \sum (O_i - \overline{O})^2]}} \qquad \text{(eq. 2.6)}$$

$$MAE = N^{-1} \sum_{i=1}^{N} | P_i - O_i | \qquad \text{(eq. 2.7)}$$

$$RMSE = N^{-1} \sum_{i=1}^{N} [(P_i - O_i)^2]^{-1/2} \qquad \text{(eq. 2.8)}$$

$$d = \frac{N * RMSE^2}{\sum_{i=1}^{N}(| P_i - \overline{O} | + | O_i - \overline{O} |)^2} \qquad \text{(eq. 2.9)}$$

$$RE = \frac{\sum_{i=1}^{N}[(P_i - O_i) / O_i]}{N} * 100 \qquad \text{(eq. 2.10)}$$

where O is the observed data, P is the model prediction, N is the number of observations, and i is the day. Graphical analysis was also done as systematic biases are often revealed more clearly through graphs than statistics.

2.4 Results and Discussion

The primary objective of this section is to assess model estimations for SWE and soil temperature; however, air temperature must also be considered because it dictates precipitation routing and soil temperature calculation.

2.4.1 Air Temperatures and Lapse Rates

The linear extrapolation used by MT-CLIM to model daily maximum and minimum air temperature is well correlated with *in situ* measurements recorded at the four sites in the Rattlesnake (Table 2.2). Simulated maximum daily air temperature is slightly more accurate than model results for minimum daily air temperature. Additionally, model effectiveness seems to decline with increasing elevation.

Measure-ment, Station	Elev. (m)	Obs. Mean (°C)	Obs. Std. Dev.	Pred. Mean (°C)	Pred. Std. Dev.	MAE	RMSE	d	RE (%)	Pearson's r	p	n
Tmin, Stuart Peak	2215	-1.8	7.6	-2.9	7.6	3.1	4.0	0.93	-63.7	0.87	< 0.05	4653
Tmax, Stuart Peak	2215	6.6	9.3	6.4	11.5	4.1	5.3	0.93	-28.1	0.89	< 0.05	4653
Tmin, Woods Gulch	1491	-0.8	7.2	-1.2	7.1	2.4	3.0	0.95	-21.4	0.91	< 0.05	224
Tmax, Woods Gulch	1491	7.2	9.4	10.3	10.5	3.8	4.2	0.96	81.4	0.97	< 0.05	224
Tmin, Rattelsnake Moraine	1205	-3.2	6.0	-3.2	6.0	1.2	1.5	0.98	30.5	0.97	0.88	189
Tmax, Rattelsnake Moraine	1205	6.0	8.3	7.3	8.7	1.9	2.2	0.98	50.5	0.98	< 0.05	189
Tmin, Missoula 2NE	1046	1.0	7.4	0.3	7.9	1.3	1.7	0.99	-24.7	0.98	< 0.05	14802
Tmax, Missoula 2NE	1046	13.8	11.3	13.3	11.8	1.0	1.5	1.00	-11.1	0.99	< 0.05	14801

Table 2.2 Statistical results comparing BIOME-BGC 4.2 predictions with *in situ* measurements for daily minimum and maximum temperature at the meteorological stations in the Rattlesnake Creek watershed.

Diurnal temperature variability in the Missoula valley is complicated by cold air drainage and temperature inversions, which generally occur at night (Finklin, 1984; Geiger et al., 2003). This phenomenon results in temperature transects that do not adhere to the simple parameterized lapse-rate in MT-CLIM, and likely explains why the model is more effective at predicting daily maximum temperature and temperatures at lower elevations. Lapse rates calculated from observations for the Missoula area (Table 2.3) reinforce this idea, particularly during the winter months when SWE estimations are most affected. However, when locally calculated lapse rates replaced the normal, default lapse rate used in MT-CLIM the change resulted in increased error in SWE calculations. Therefore, the default lapse rate of -6°C/km for daily maximum temperature and -3°C/km for daily minimum temperature were used throughout the study.

	T_{min} (°C/km)	T_{max} (°C/km)
Winter	-1.9	-3.6
Spring	-2.4	-6.7
Summer	-2.9	-7.9
Fall	-1.4	-5.8

Table 2.3. Lapse rates calculated between the airport and Stuart Peak SNOTEL for daily maximum and minimum air temperature.

2.4.2 Soil Temperature

Predicted daily soil temperature at the Wood's Gulch and Rattlesnake Moraine sites are correlated with measured soil temperature, however, the relative error in BIOME-BGC output is extremely high (Table 2.4). It appears that most of the modeling error occurs as an over-prediction of soil temperature when there is snow present; however, soil temperature also appears to be underestimated during warm conditions. Graphical analysis supports this (Figure 2.5) and suggests there may be a systematic error in modeling soil temperature stabilization during periods of snow due to algorithm neglect of snow presence (Figure 2.5d).

Similarly, other researchers (Lagergren et al., 2006) have found model overestimation of soil temperature by BIOME-BGC (v4.2) when snow is present. The isolation qualities of snow tend to dampen soil heat flux (Bayard et al., 2005). Some research, drawing on *in situ* measurements taken in the arctic, suggests that soil temperature become decoupled from air temperature with increased snow depth, eventually entering a regime where the soil-snow interface temperature becomes a function of soil moisture, ground heat flux and earlier winter air temperatures (Taras et al., 2002).

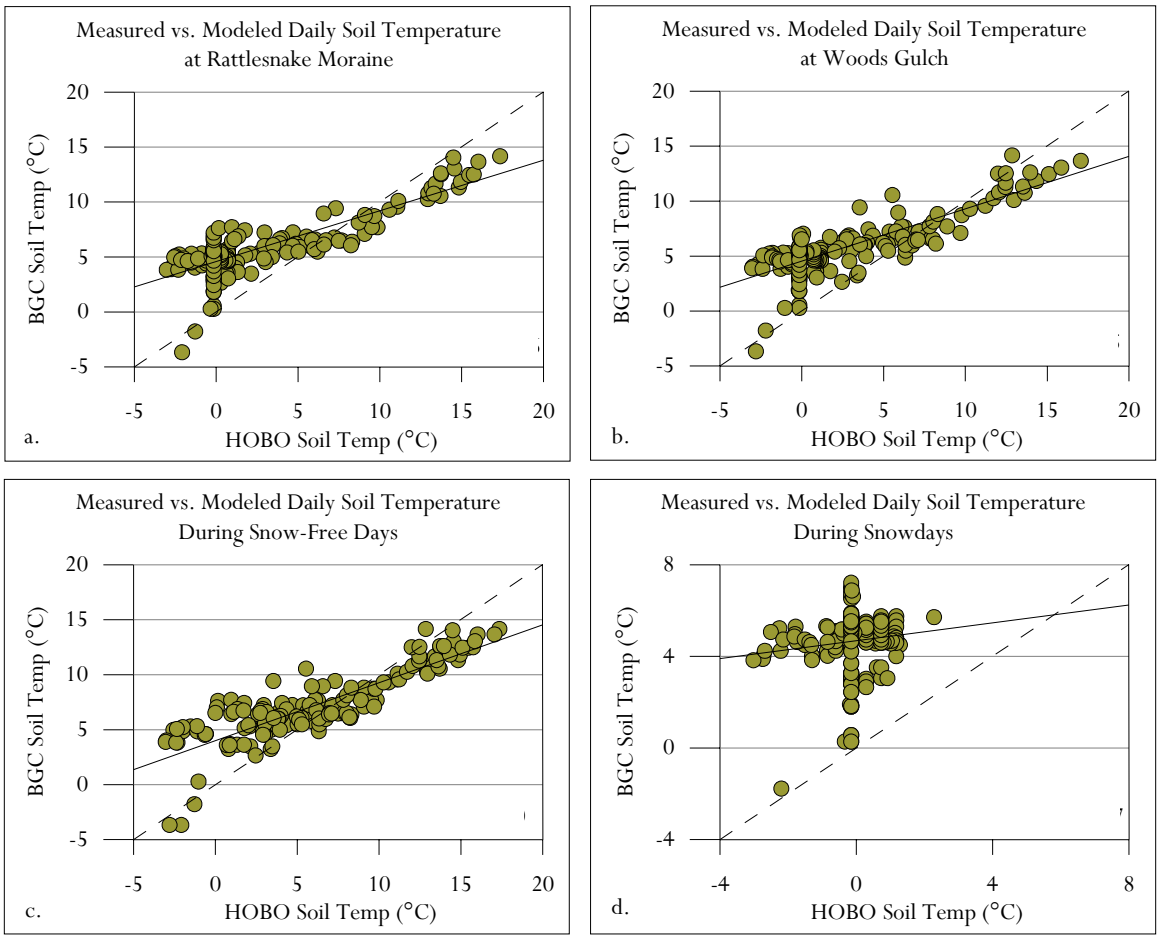

Figure 2.5. Graphs comparing measured and modeled soil temperature at the Rattlesnake Moraine (a) and Woods Gulch (b) sites. Site data was combined to compare snow-free (c) periods with snow days (d). The dashed line represents a one-to-one relationship.

Site	Obs. Mean (°C)	Obs. Std. Dev.	Pred. Mean (°C)	Pred. Std. Dev.	MAE	RMSE	d	RE (%)	Pearson's r	p	n
Rattlesnake Moraine	2.5	4.7	5.7	2.6	3.9	4.4	0.75	376.2	0.83	<0.01	190
Woods Gulch	2.6	4.4	5.8	2.6	3.7	4.2	0.75	246.7	0.82	<0.01	181
Snow-free Days	6.1	5.1	7.2	3.1	2.4	3.1	0.85	139.8	0.86	<0.01	159
Snow Days	-0.1	0.8	4.7	1.3	4.8	5.0	0.15	763.6	0.12	<0.01	213

Table 2.4. Statistics comparing measured and modeled soil temperature (°C) at the Rattlesnake Moraine and Woods Gulch sites. Site data was combined to compare snow-free periods with snow days.

2.4.3 Daily and Peak Annual SWE

Comparing validation statistics for SWE is problematic because of differences in the validation data. However, the differences between the *in situ* measurements could also illuminate some of the model's shortcomings. Statistically, the simplistic snow model in BIOME-BGC predicts daily SWE adequately at the Stuart Peak SNOTEL site (Table 2.5). Comparing the statistics for the SNOTEL and snow course data suggests the model predicts peak SWE less effectively (Table 2.5).

Graphical analysis of the snow course data implies BIOME-BGC over-predicts peak SWE (Figure 2.6). However, the comparison between BIOME-BGC output and SNOTEL measurements indicate model under-prediction of peak SWE for most years. Model results for the 1996-1997 snow year were anomalous, resulting in a significant over-prediction of peak SWE that caused modeled snowpack to persist well beyond the observed melt date (Figure 2.7 and Figure 2.8). Figure 2.8 suggests that the ability of the model to predict peak SWE accurately is partially dependant upon the amount of precipitation received at the base station (here, the airport).

The SNOTEL record is restricted to the late 20th century, a period plagued by drought-like conditions (Figure 2.9). This potential explanation in the over-prediction of peak SWE during wet years is supported when one compares the Stuart Peak snow course measurements, a record that precedes the current drought conditions, taken before and after the installation of the SNOTEL (Figure 2.6a).

TV Mountain offers an alternative explanation. The snow course measurements taken at TV Mountain are over-predicted throughout the period of record (Figure 2.6b),

suggesting that the under-estimation at Stuart Peak since 1996 could be the result of non-climatic drivers, such as increased forest canopy, and not due to changes in precipitation.

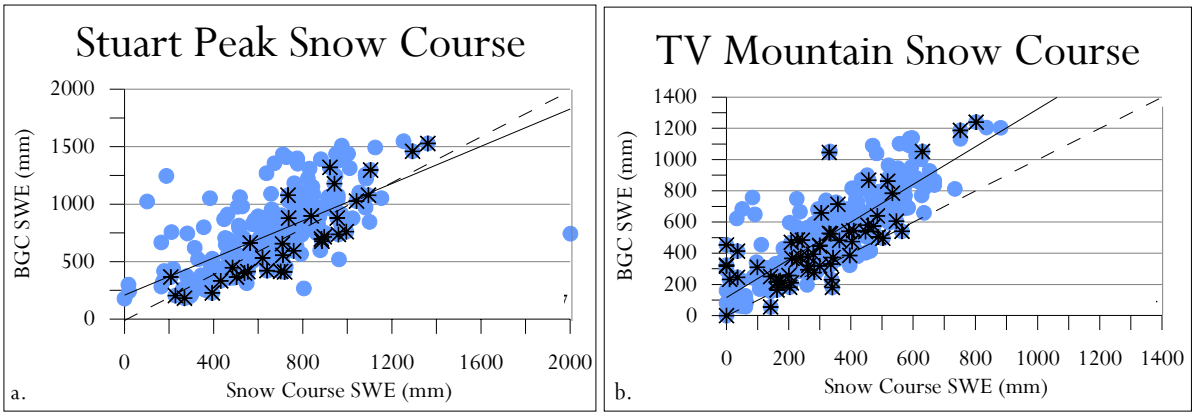

Figure 2.6. Scatterplot of BIOME-BGC estimations of SWE and snow course measurements taken at Stuart Peak since 1937 (a) and TV Mountain since 1956 (b). Stared data points represent measurements taken since 1996, the year the Stuart Peak SNOTEL was installed. Dashed line shows a one-to-one relationship. Axes are fitted to data at each site.

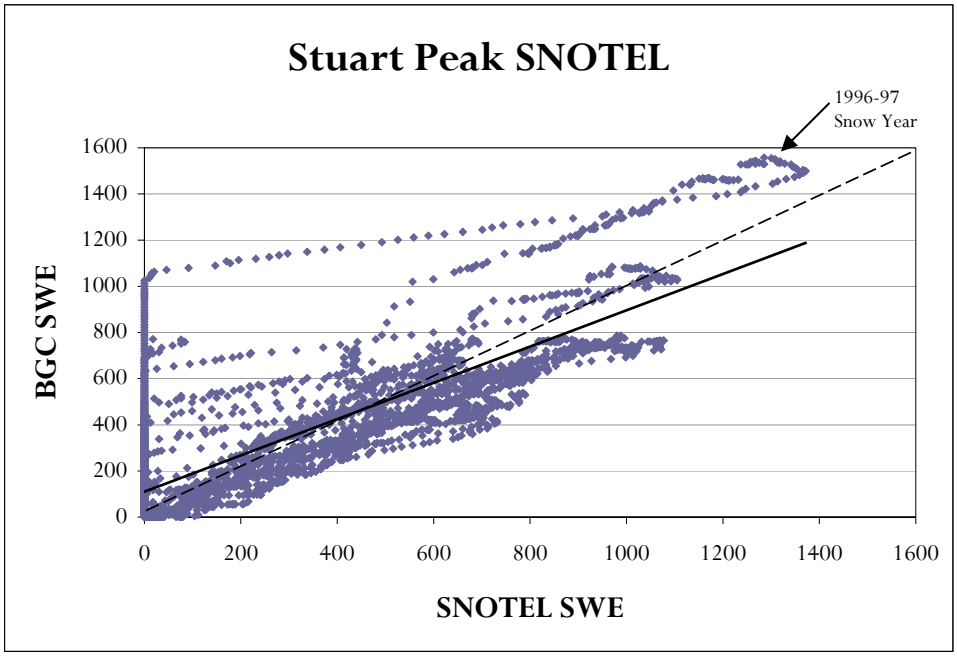

Figure 2.7. Scatterplot of measured and modeled daily SWE at the Stuart Peak SNOTEL. Dashed line shows a one-to-one relationship

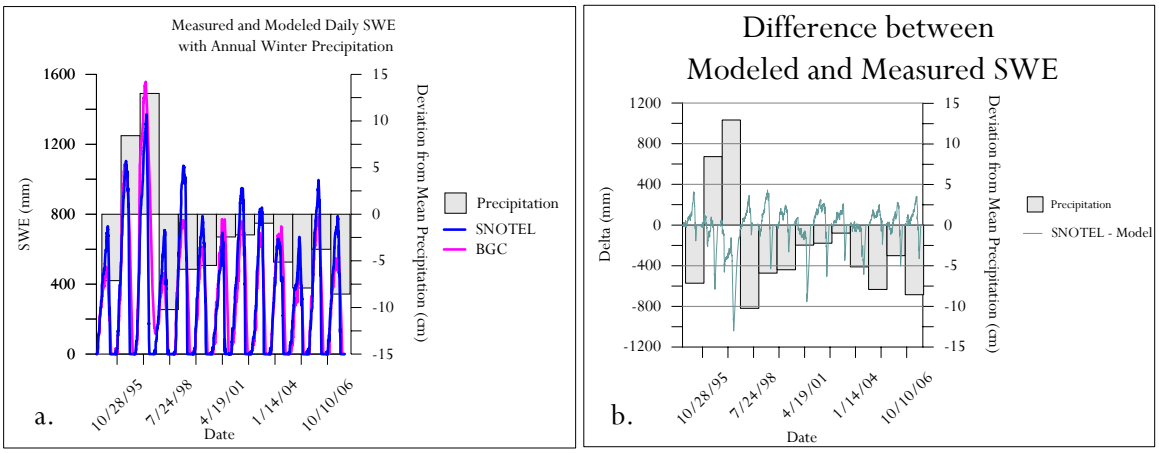

Figure 2.8. Graph showing (a) simulated and measured daily SWE at the Stuart Peak SNOTEL site and (b) the difference of those two, overlaid with annual winter precipitation recorded at the Airport. Negative values in (b) represent model over-prediction of SWE.

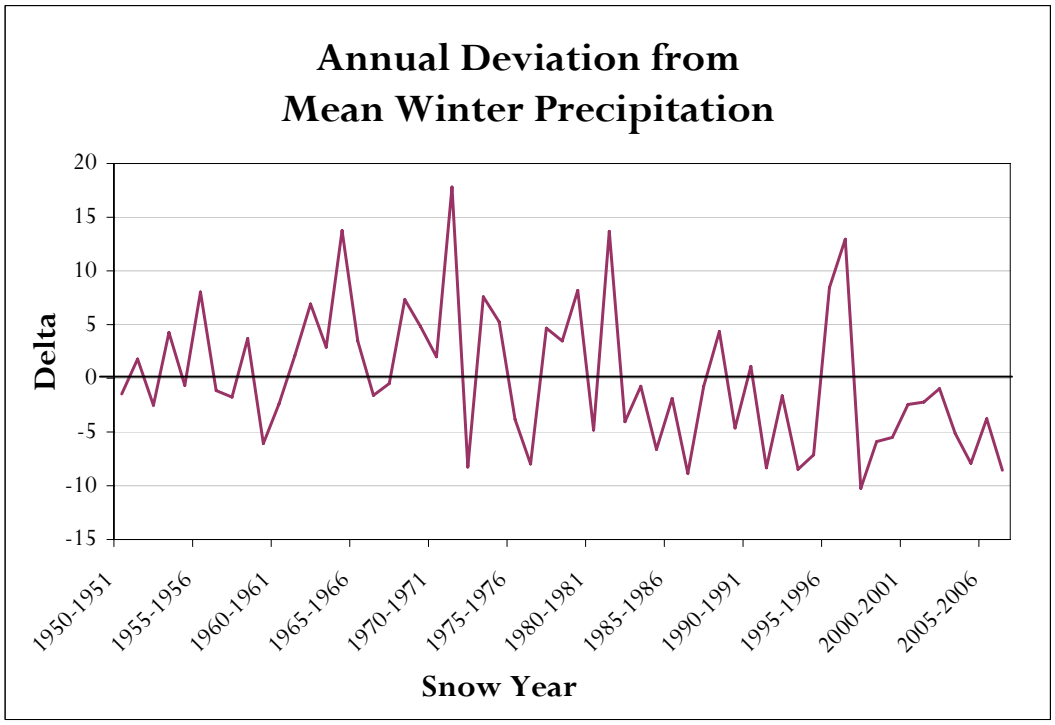

Figure 2.9. Annual difference between total winter precipitation and mean winter precipitation (cm) measured at the Airport (1950-2006).

Measurement, Station	Observed Mean (mm)	Standard Deviation	Predicted Mean (mm)	Standard Deviation	MAE	RMSE	d	RE (%)	Pearson's r	p	n
All Data Stuart Peak SNOTEL	322.9	340.3	342.9	337.2	113.2	184.9	0.92	56.7	0.85	<0.05	4745
Non-Zero Stuart Peak SNOTEL	400.0	335.6	424.7	325.8	140.3	205.8	0.90	56.7	0.81	<0.05	3831
Stuart Peak Snow Course	663.9	267.0	744.8	326.1	186.7	261.7	0.79	32.5	0.66	<0.05	238
TV Mountain Snow Course	343.1	173.7	530.5	257.4	192.3	242.2	0.73	86.4	0.81	<0.05	297
Woods Gulch, Soil Temp	--	--	--	--	--	--	0.82	-22.0	*0.65*	<0.05	181
Rattlesnake Moraine, Soil Temp	--	--	--	--	--	--	0.81	-26.8	*0.65*	<0.1	190

Table 2.5 Statistical results comparing BIOME-BGC, v4.2 SWE calculations with *in situ* measurements. Daily soil temperature is used as a surrogate to indicate snow presence at the Woods Gulch and Rattlesnake Moraine sites.

2.4.4 Snowpack Evolution

Snow-course measurements are manually taken near the end of the snow season and, therefore, are only useful for predicting late season model performance. SNOTEL and COOP measurements, on the other hand, are taken continuously and can be used to assess how the model handles snowpack evolution and development. Predicted snow days are well correlated, but dramatically overestimated compared to COOP observations (Figure 2.10). The model is more than 30 days in error at the SNOTEL site and more than three weeks in error at the COOP site (Table 2.6).

Statistics and figures of snowpack evolution suggest that BIOME-BGC effectively predicts the onset of the snow season (Table 2.6, Figure 2.11), but is less successful at simulating snow melt (Table 2.6, Figure 2.12). The comparison between snow course measurements and BIOME-BGC output suggests the model is over-predicting late season snowpack, which is also the case at the SNOTEL site. The failure of the model to predict the date of melt and the apparent over-prediction of late-season snowpack may be the result of an inadequate melt algorithm.

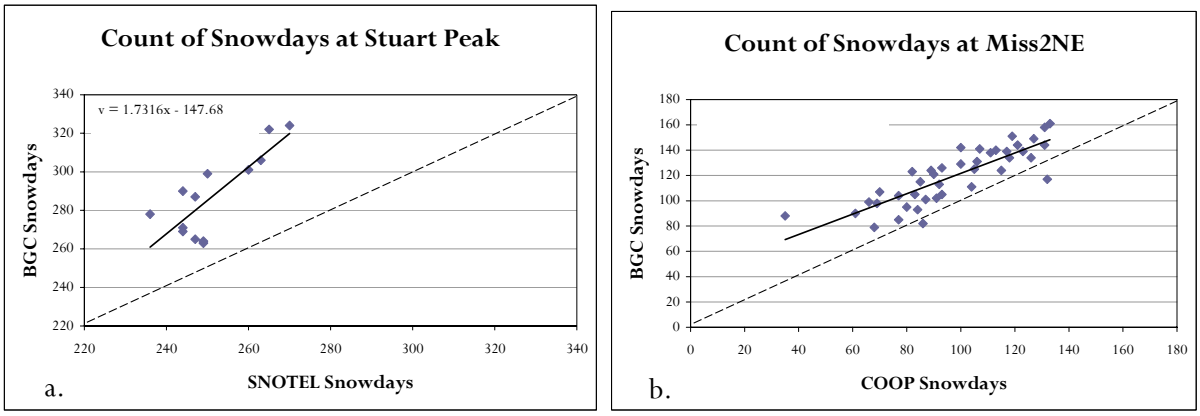

Figure 2.10. Modeled annual snowdays are over-predicted at both (a) the high-elevation SNOTEL site and (b) the low elevation COOP station.

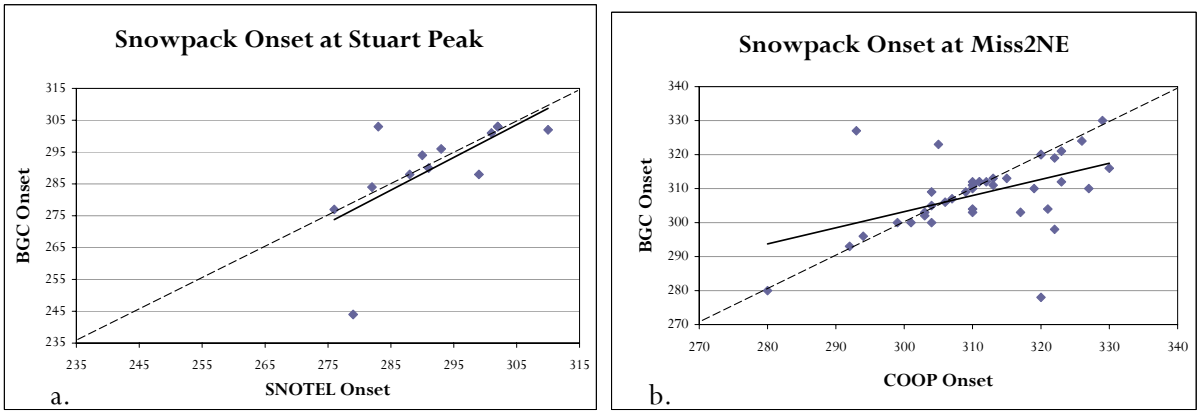

Figure 2.11. Observed and predicted data for snowpack onset at both (a) Stuart Peak and (b) Miss2NE.

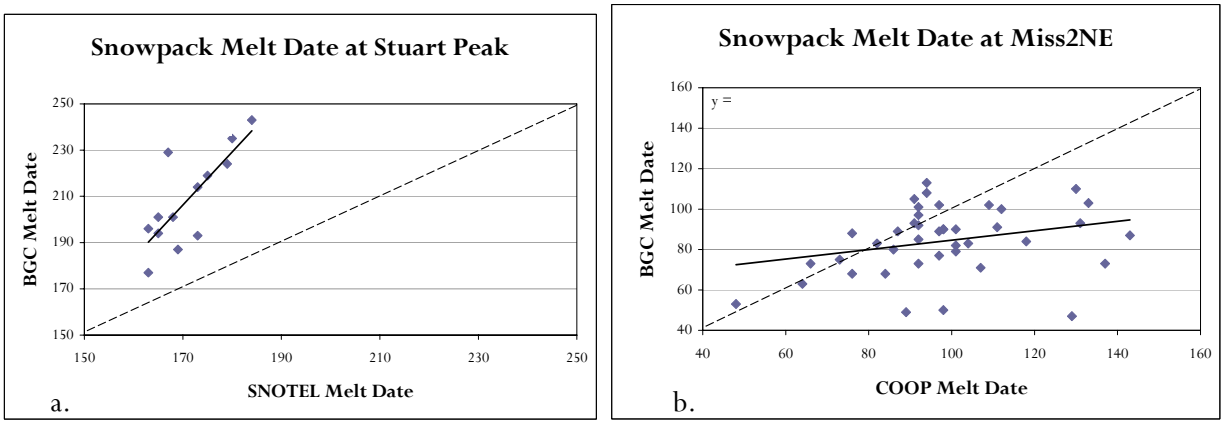

Figure 2.12. Observed and predicted data for melt date at (a) Stuart Peak and (b) Miss2NE.

Station, Measurement	Obs. Mean	Obs. Std. Dev.	Pred. Mean	Pred. Std. Dev.	MAE	RMSE	d	RE (%)	Pearson's r	p	n
Stuart Peak, Snow Days	251.4	10.0	287.6	21.5	36.2	38.9	0.41	14.3	0.80	0.15	13
Stuart Peak, % Snow Days	93.1	4.0	97.3	3.1	4.5	5.7	0.57	4.7	0.38	<0.05	13
Miss2NE, Snow Days	97.5	22.9	119.7	22.0	23.1	25.6	0.74	26.3	0.84	<0.05	41
Miss2NE, % Winter Snow Days	65.5	17.1	85.3	11.8	19.8	24.5	0.58	38.7	0.54	<0.05	41
Stuart Peak, Onset Date	292.0	10.3	292.5	10.0	4.4	7.0	0.87	0.2	0.74	<0.5	13
Miss2NE, Onset Date	311.2	10.8	308.5	10.8	6.0	11.2	0.71	-0.8	0.48	<0.05	41
Stuart Peak, Melt Date	173.6	10.7	208.5	28.0	39.9	44.4	0.22	20.3	0.13	>0.5	13
Miss2NE, Melt Date	97.9	20.2	84.1	16.6	18.5	25.9	0.54	-10.8	0.28	<0.05	41

Table 2.6. Statistics comparing BIOME-BGC (v4.2) snowpack evolution with *in situ* measurements.

2.5 Conclusions

Examination of SWE and soil temperature leads to several conclusions, the first being that the model appears to fail most severely during anomalously wet years. Although 1996-97 was not the wettest winter on record in the Missoula valley, the precipitation received at the airport was above average. Climatic anomalies, such as the winter of 1996-97, can significantly affect extrapolation of precipitation to remote sites when a simple linear lapse-rate is used to calculate precipitation, such as that used by MT-CLIM. Several studies (Garen et al., 1994; Garen & Marks, 2005; Susong et al., 1999) have successfully used detrended krigging to distribute precipitation across a basin; however, this method requires input from several stations measuring precipitation at varying elevation.

BIOME-BGC, v4.2 sacrifices a robust consideration of the physical principles controlling snowpack and soil temperature for simplicity within a large, complex eco-physical model. Simplifying the physics of the snowpack could partially be responsible for the inability of the model to predict peak SWE and melt the snowpack in a timely manner. Integrating new snowmelt and soil temperature algorithms in the current BIOME-BGC framework may improve model performance and is addressed in the following chapters.

Chapter 3: Potential Physical Adjustments to the BIOME-BGC SWE Subroutine

3.1 Introduction

The snow routine in BIOME-BGC sacrifices nearly all physical processes affecting the snowpack for a simple, modified degree-day snowmelt calculation. Degree-day snowmelt models are computationally simplistic and utilize easily obtainable meteorological inputs (Hock, 2003). These models have been used in a variety of locations for watersheds of varying size, landscape characteristics and elevation (Ferguson, 1999; WinSRM, 2003), including western Montana (Bleha, 2006).

More complex energy balance models are an alternative to the simplified degree-day approach. Some researchers have successfully used energy-balance calculations to predict seasonal snowpack (Anderson, 1976; Bloschl et al., 1991; Cline et al., 1998; Essery, 2003; Garen & Marks, 2005; Marks et al., 1999; Marks & Dozier, 1992; Tague & Band, 2004; Tarboton & Luce, 1996; Zanotti et al., 2004). Energy-balance models generally perform well and are able to predict detailed snowpack characteristics; however, extensive meteorological inputs and computing power usually limit them spatially and temporally (Fierz et al., 2003; Xu et al., 2004).

It is well established that snow-cover influences soil temperature (Bayard et al., 2005; Lagergren et al., 2006; Taras et al., 2002). The soil temperature algorithm in BIOME-BGC (v4.2) neglects the influence of snow cover on soil temperature.

This chapter conceptualizes and evaluates several physical parameters that could be incorporated into the current snowmelt routine within BIOME-BGC, resulting in a combined degree-day and partial energy-balance algorithm. Each algorithm was chosen

to easily fit in the broader framework of BIOME-BGC while addressing the issues with estimating peak SWE and the melt date. Additionally, an extension of the soil temperature algorithm was evaluated. The goal of this analysis was to improve the soil temperature sub-routine and to adjust the snow model in BIOME-BGC so it can predict peak SWE and attributes related to snowpack evolution with better accuracy. Model evaluation was performed only on the soil temperature and snow routines, calculated outside the larger BIOME-BGC framework. The cascading effects of the calculations and resulting perturbation to the ecosystem model were not examined in this study.

3.2 Methods

Five adjustments were proposed, evaluated using model statistics, and assessed for performance. Details of each are described separately in the following sections.

3.2.1 Soil Temperature

Lagergren et al. (2006) developed a new algorithm for BIOME-BGC that used modeled SWE accumulation as a soil temperature dampening factor. The algorithm,

$$T_{soil} = T_{ra} + (0.2 + \frac{0.8*SWE}{5 + SWE}) * (0.5 - T_{ra}) \qquad \text{(eq. 3.1)}$$

where T_{ra} is an 11-day running average of the mean daily temperature, was evaluated using data from the Rattlesnake Moraine and Woods Gulch sites. An adjustment was made to the Lagergren et al. (2006) algorithm to incorporate the decoupling effect that snow has on soil temperature and air temperature. The modified Lagergren algorithm assumes the soil temperature remains constant at 0°C when snow is present, such that

$$T_{soil} = T_{ra} + (0.2\ (0.5 - T_{ra})) \text{ for snow-free periods, and} \qquad \text{(eq. 3.2)}$$
$$T_{soil} = 0 \text{ for snow days.}$$

3.2.2 Albedo Decay

Variability in snow albedo is important to radiation-driven ablation (Coughlan & Running, 1997). Albedo decay can be calculated as a function of temperature (Coughlan & Running, 1997) or age of snowpack (Jordan, 1991; Stahli & Jansson, 1998; Tague & Band, 2004; Tarboton & Luce, 1996). The albedo decay function tested here was based on the work of Tague and Band (2004). It was adjusted to fit within the larger BIOME-BGC framework such that:

$$\alpha = 0.85\ (0.82^{Age^{0.46}}) \text{ for } T_{day} \geq 0, \text{ and} \qquad \text{(eq. 3.3)}$$
$$\alpha = 0.85\ (0.94^{Age^{0.58}}) \text{ for } T_{day} < 0$$

where "Age" is the days since the last snowfall. This function was chosen for evaluation because it is used in RHESSys, a similar eco-physical model (Tague & Band, 2004), and is easily incorporated into BIOME-BGC. The equation should increase snowmelt as the snowpack ages, which will potentially cause an increase in peak SWE and an earlier melt date.

3.2.3 Canopy Interception

Interception of falling snow by the forest canopy can significantly reduce snow accumulation on the ground (Pomeroy & Gray, 1995; Stottlemyer & Troendle, 2001; Strasser et al., 2007; Troendle et al., 2001). BIOME-BGC accounts for canopy interception of rainfall, but not snow (Thornton, 1998). Canopy interception is modeled

here as a function of the leaf area index (LAI) and a dimensionless unloading coefficient (Pomeroy et al., 1998), so that:

$$I = I_{t-1} + 0.7(I_{max} - I_{t-1})(1 - e^{(-P/I_{max})}), \quad \text{(eq. 3.4)}$$

where I_{t-1} is the accumulated snow interception from the previous day, I_{max} is the maximum intercepted snow, P is SWE that fell in the current time-step. I_{max} is equal to 4.4 * LAI (Hedstrom & Pomeroy, 1998); daily projected LAI, calculated by BIOME-BGC (Thornton, 1998), is used for calculating I_{max}. Addition of a canopy interception equation will likely decrease peak SWE, resulting in an earlier melt date.

3.2.4 Rain-On-Snow

Advected heat transfer from rain-on-snow events can change the energy of the snowpack considerably (Male & Gray, 1981; Upadhyay, 1995; Xu et al., 2004). This study examined the addition of the melt calculation used by RHESSys (Tague & Band, 2004),

$$M_v = (\rho_{water} * T_{air} * TF * cp_{water}) / \lambda_{f,} \quad \text{(eq. 3.5)}$$

where ρ_{water} is the density of water, TF is throughfall, cp_{water} is the heat capacity of water and λ_f is the latent heat of fusion. Since rain-on-snow events occur more frequently in the spring, the addition of this equation should cause the snow to melt earlier but leave peak SWE largely unaffected.

3.2.5 Mixed Precipitation

Many snow models calculate mixed precipitation events based on a temperature or dew-point threshold (Jordan, 1991; Marks et al., 1999; Tarboton & Luce, 1996). The temperature index proposed by Marks et al. (1999) is added to BIOME-BGC such that,

$$\begin{aligned} -0.5°C > T_{min}&, 100\% \text{ Precipitation} = SWE, \\ -0.5°C < T_{min} < 0°C&, 75\% \text{ Precipitation} = SWE, \\ 0°C < T_{min} < 0.5°C&, 25\% \text{ Precipitation} = SWE, \\ 0.5°C < T_{min}&, 0\% \text{ Precipitation} = SWE. \end{aligned} \qquad \text{(eq. 3.6)}$$

The mixed precipitation algorithm will likely cause an increase in predicted peak SWE, which will result in a later melt date if no adjustment is made to the snowmelt equation.

3.2.6 Model Evaluation

Model results for SWE were assessed using the Stuart Peak SNOTEL data and soil temperature estimations are compared to the Rattlesnake Moraine and Woods Gulch sites. Results will be evaluated using the same statistical methods described in Chapter 2. All algorithms changes were considered individually and holistically.

3.3 Results and Discussion

The impact of the proposed adjustments on soil temperature, SWE estimates and snowpack evolution are discussed in the following sections.

3.3.1 Soil Temperature

Both soil temperature adjustments show improvement over the algorithm inherent in BIOME-BGC (v4.2; Table 2.4), especially on snow days (Table 3.1). The modified Lagergren algorithm appears statistically superior to the original Lagergren algorithm on snow days; however, there appears to be room for further improvement. Examination of scatter-plots of the predictions corroborates the statistical evidence that both algorithms are an improvement over BIOME-BGC (v4.2; Figures 3.1 and 2.2). The graphs of soil temperatures over time suggest that the modified Lagergren algorithm may fail during periods of shallow snowpack (Figure 3.2). Error can also accumulate in the model because the algorithm for soil temperature refers to the SWE predicted by BIOME-BGC (v4.2).

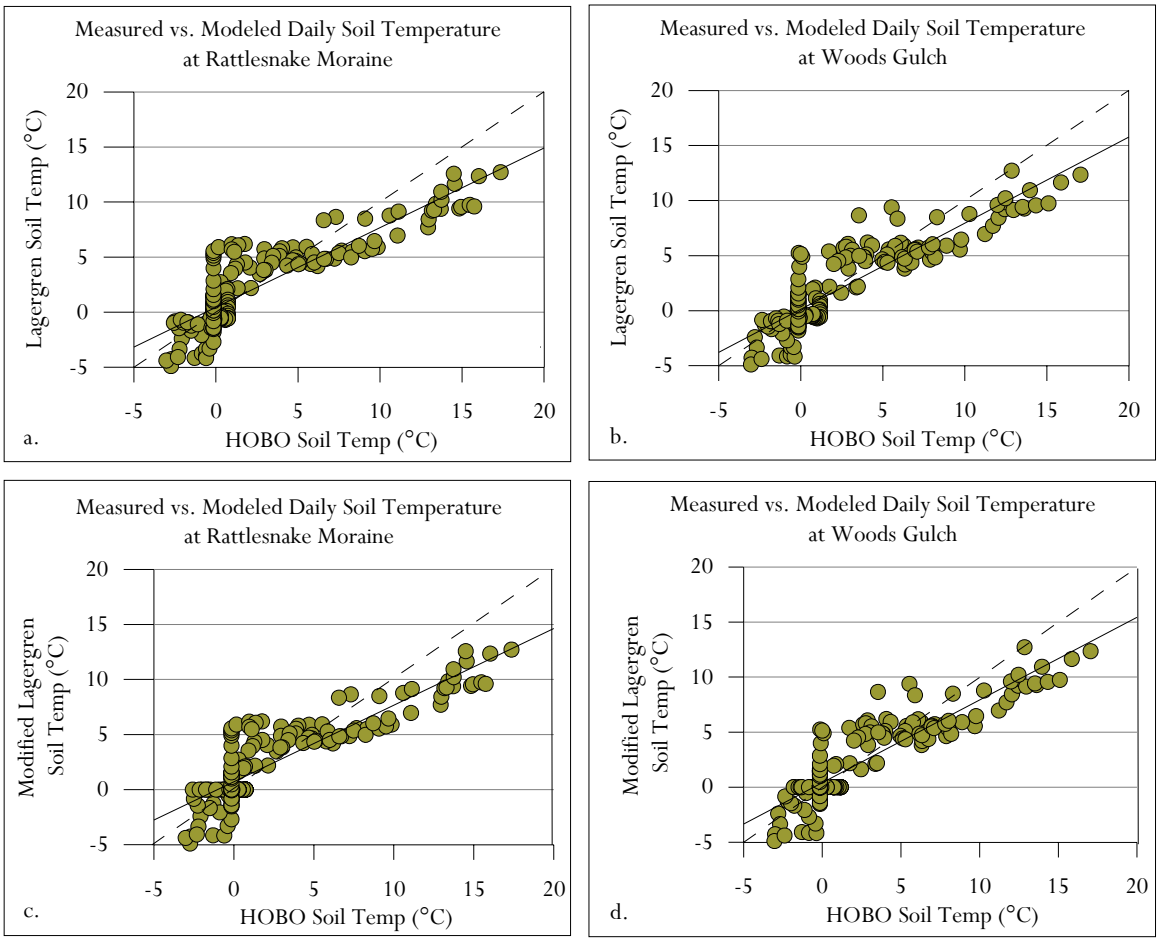

Figure 3.1. Scatterplots comparing measured and modeled soil temperature at the Rattlesnake Moraine (a & c) and Woods Gulch (b & d) sites. Both the Lagergren (a & b) and modified Lagergren (c & d) were evaluated.

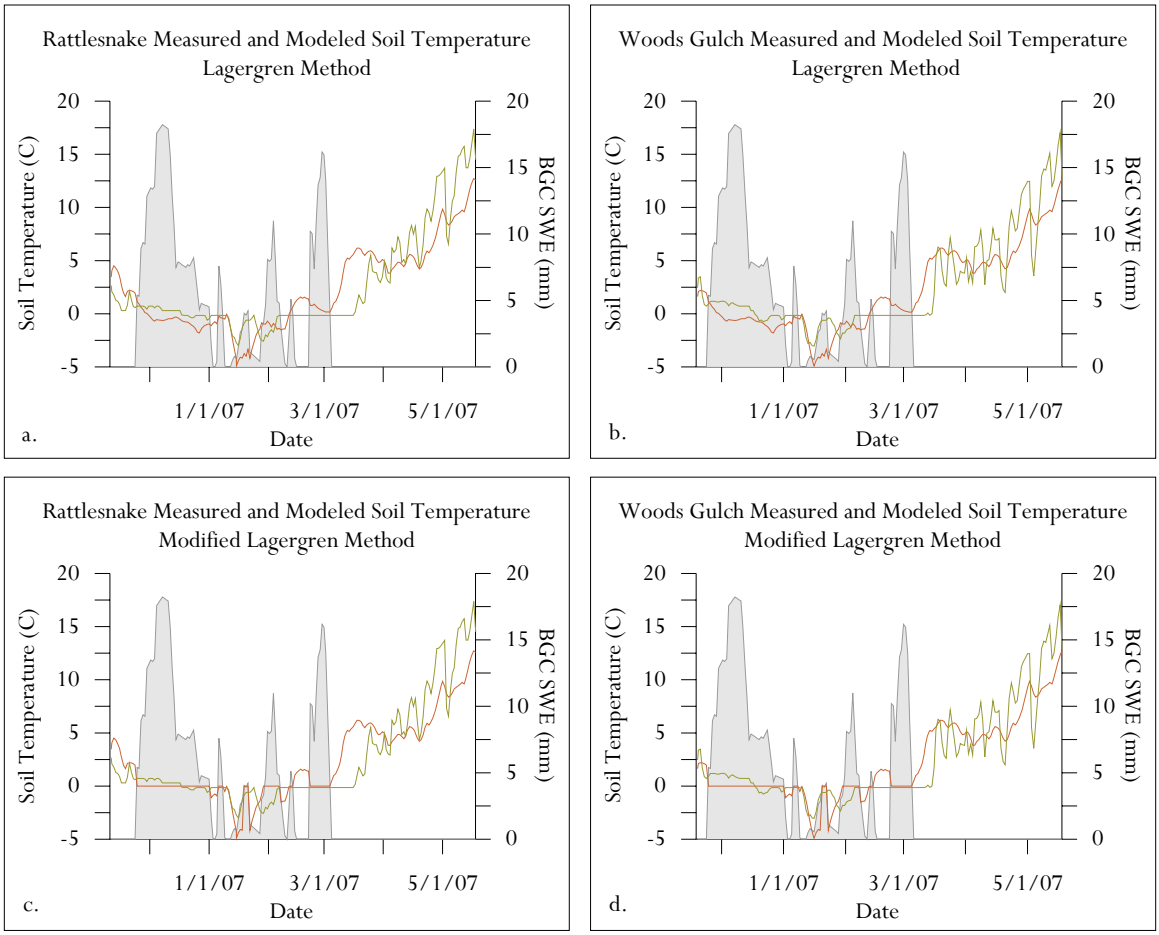

Figure 3.2. Time-series graph of measured and modeled soil temperature at the Rattlesnake Moraine (a & c) and Woods Gulch (b &d) sites. Both the Lagergren (a & b) and modified Lagergren (c & d) are tested. The green line represents measured soil temperature, red is modeled soil temperature and the grey area is daily SWE modeled by BIOME-BGC (v4.2).

	Obs. Mean (°C)	Std. Dev.	Prd. Mean (°C)	Std. Dev.	MAE	RMSE	d	RE (%)	Pearson's r	p	n
Rattlesnake Moraine, Lagergren	2.5	4.7	2.2	3.9	1.8	2.3	0.92	46.1	0.87	<0.01	190
Rattlesnake Moraine, Modified Lagergren	2.5	4.7	2.4	3.7	1.6	2.3	0.92	63.3	0.88	<0.01	190
Woods Gulch, Lagergren	2.6	4.4	2.1	3.9	1.6	2.0	0.94	33.1	0.89	<0.01	181
Woods Gulch, Modified Lagergren	2.6	4.4	2.3	3.7	1.5	2.0	0.94	42.2	0.90	<0.01	181
Snow-free Days	6.1	5.1	5.4	3.6	2.2	2.7	0.90	85.6	0.87	<0.01	159
Snow Days, Lagergren	-0.1	0.9	-0.2	1.9	1.3	1.7	0.47	578.2	0.37	<0.5	213
Snow Days, Modified Lagergren	-0.1	0.8	0.0	0.0	0.6	0.9	0.12	97.9	n/a	n/a	213

Table 3.1. Statistics comparing measured and modeled soil temperature at the Rattlesnake Moraine and Woods Gulch sites. Data from the two sites was combined to compare snow days with snow-free days. There was no difference between the Lagergren and modified Lagergren algorithm during snow-free periods.

3.3.2 Daily and Peak SWE

None of the physically based algorithm adjustments show marketable statistical improvement over the ability of BIOME-BGC (v4.2) to predict daily SWE (Table 3.2). The few statistical measures that were improved showed only slight improvement. Most of the physical adjustments were statistically worse than or equal to BIOME-BGC (v4.2).

Graphically, some of the physical parameters show slight improvement over BIOME-BGC (v4.2) for the prediction of daily SWE (Figure 3.3). The linear regression (slope) between measured and modeled daily SWE is improved for all the physical adjustments added to BIOME-BGC except canopy interception (Figure 3.3). The physically based adjustments follow the same basic pattern as the original model,

generally under-predicting SWE during peak accumulation and over-predicting SWE at the end of the season (Figure 3.4). None of the algorithms tested here correct the inability of BIOME-BGC (v4.2) to completely melt SWE at the end of the 1996 snow year (Figure 3.4), resulting in an erroneously modeled perennial snowpack that is most pronounced when all the physical parameters are combined (Figure 3.4f). Canopy interception shows the best results for adjusting late season SWE, but the model still grossly under-predicts the melt rate (Figure 3.4c).

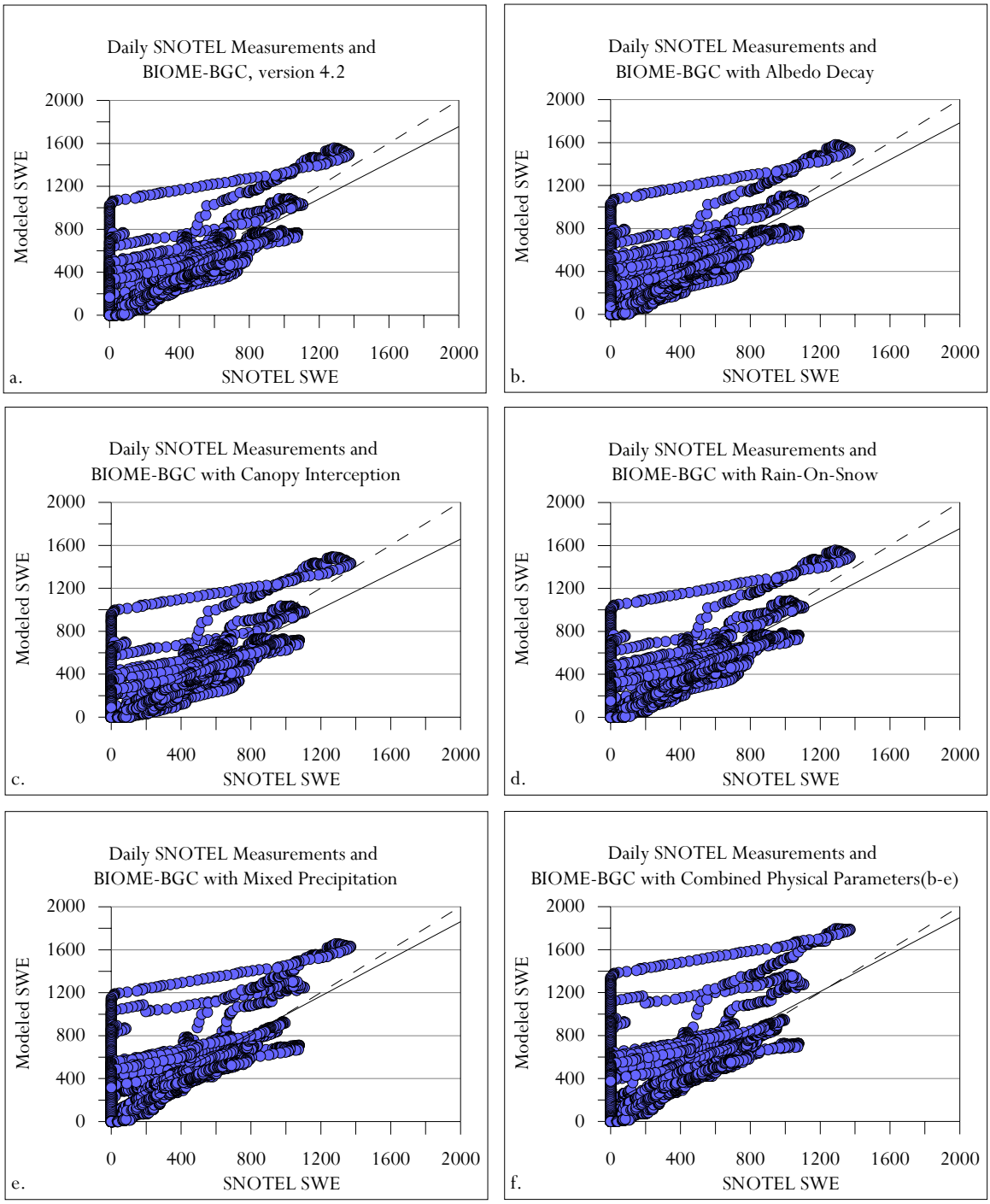

Figure 3.3. Scatterplots of predicted and measured daily SWE at the Stuart Peak SNOTEL for BIOME-BGC (v4.2) and BIOME-BGC with the inclusion of physical parameters. The dashed line represents a one-to-one relationship. The solid line is the linear regression between the predicted and measured SWE.

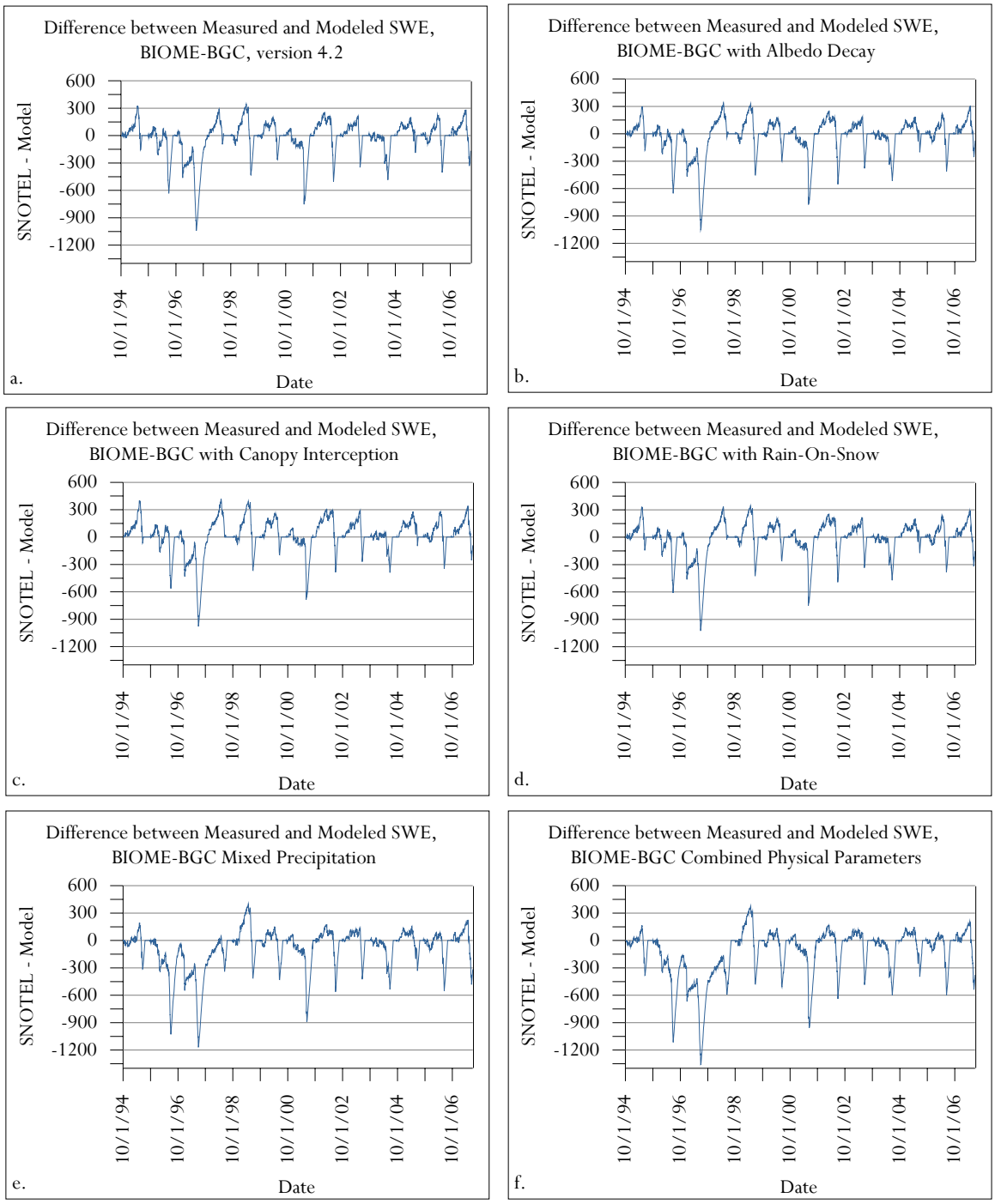

Figure 3.4. Time series graphs illustrating the difference between the measured and modeled daily SWE at the Stuart Peak SNOTEL using BIOME-BGC (v4.2) and BIOME-BGC with the addition of physically based algorithms. Negative values represent model over-prediction; positive values are under-prediction.

Model	Predicted Mean (mm)	Standard Deviation	MAE	RMSE	d	RE (%)	Pearson's r	p
4.2	342.0	327.2	113.2	184.9	0.92	56.7	0.85	<0.01
Albedo Decay	352.0	344.2	117.6	190.1	0.92	53.3	0.85	<0.01
Mixed Precip	407.7	366.3	140.1	235.5	0.89	120.5	0.81	<0.01
Canopy Interception	308.6	323.8	120.7	184.3	0.92	34.2	0.85	<0.01
Rain On Snow	343.3	337.5	114.5	183.7	0.92	50.1	0.85	<0.01
All Parameters	457.7	390.8	179.5	291.6	0.84	167.9	0.75	<0.01

Table 3.2. Validation statistics comparing BIOME-BGC, v4.2 daily SWE at Stuart Peak SNOTEL with the potential physically based model adjustments (n = 4745). The observed mean for daily SWE at the Stuart Peak SNOTEL is 322.9mm, with a standard deviation of 340.3mm.

Evaluating model response to peak SWE is more difficult than daily SWE because of the limited number of years (n = 13) that SNOTEL data is available. The addition of the physical adjustments has mixed results, improving some statistical measures while degrading others (Table 3.3). Mixed precipitation produces the best statistical results over BIOME-BGC (v4.2), with a mean predicted peak SWE that is less than 25 mm different from that measured at the SNOTEL. Including the algorithm for albedo decay and the combination of all the physical parameters generally weakens the ability of the model to predict peak SWE.

Graphical analysis reiterates the idea that all versions of the model under-predict peak SWE (Figure 3.5). Mixed precipitation, again, appears to out-perform the other physically based adjustments (Figure 3.5d). Inclusion of the canopy interception algorithm accentuates the problem with peak SWE under-prediction (Figure 3.5e).

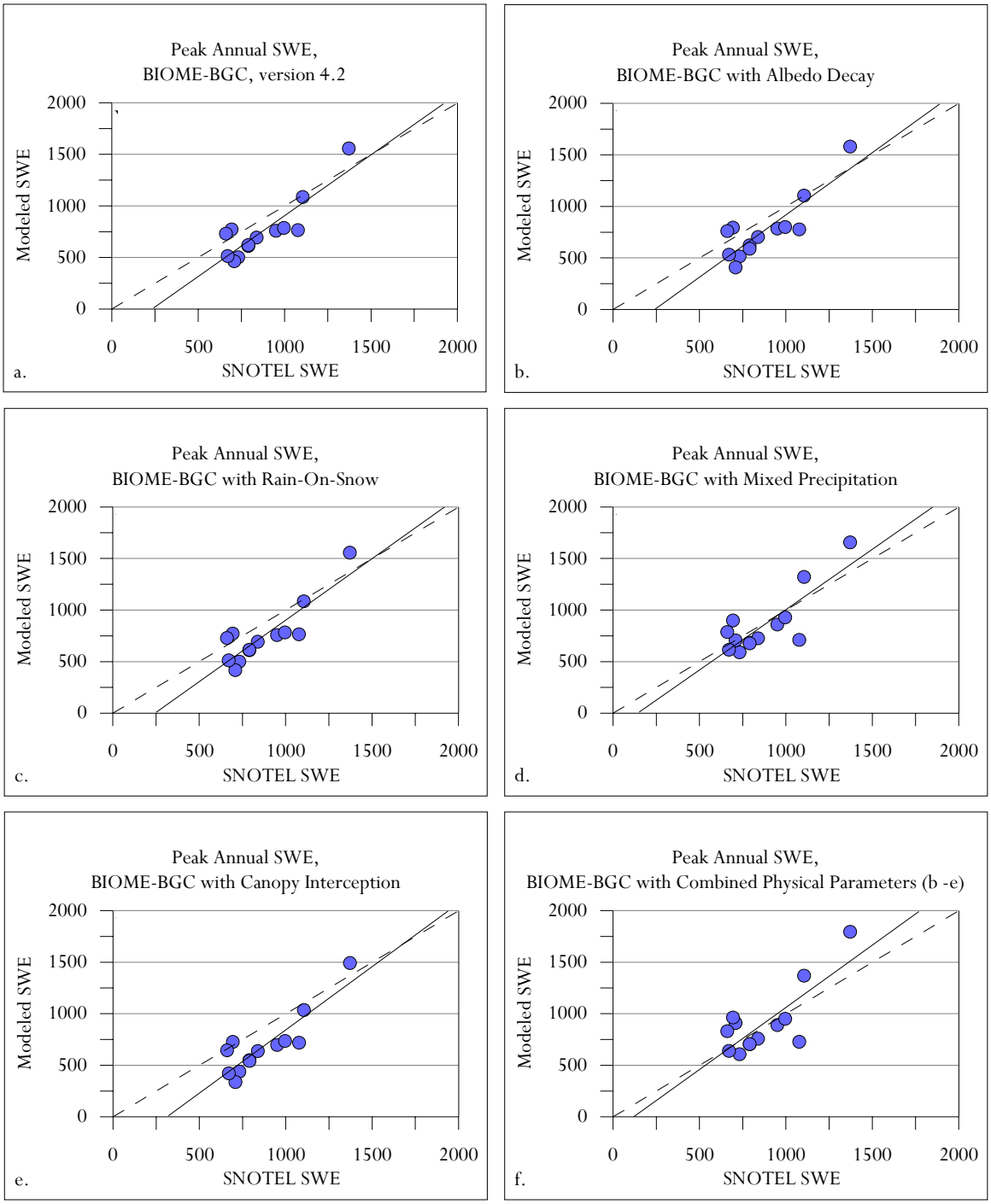

Figure 3.5. Scatterplots of predicted and measured peak annual SWE at the Stuart Peak SNOTEL for BIOME-BGC (v4.2) and BIOME-BGC with the inclusion of physical parameters. The dashed line represents a one-to-one relationship. The solid line is the linear regression between the predicted and measured SWE.

Maximum SWE	Pred. Mean (mm)	Std. Dev.	MAE	RMSE	d	RE (%)	Pearson's r	p
BIOME-BGC v4.2	758.4	289.5	168.6	184.6	0.86	-9.6	0.87	<0.5
Albedo	767.3	300.3	171.4	188.4	0.86	-8.9	0.86	<0.1
Canopy Interception	690.7	299.1	208.5	236.2	0.80	-16.6	0.87	<0.1
Rain On Snow	753.5	293.7	173.1	190.7	0.85	-10.2	0.87	<0.5
Mixed	858.6	305.4	145.1	173.8	0.87	0.7	0.82	<0.5
All Parameters	911.5	330.4	168.4	206.8	0.84	6.6	0.78	>0.5

Table 3.3. Validation statistics comparing peak annual SWE calculated by BIOME-BGC, v4.2 at the Stuart Peak SNOTEL against several potential model adjustments (n=13). The observed mean peak annual SWE at the Stuart Peak SNOTEL is 875.5 mm with a standard deviation of 213.2 mm.

3.3.3 Snowpack Evolution

Like peak SWE, evaluation of model response to snowpack evolution is difficult because of the limited number of years that SNOTEL data is available. Snowpack onset is slightly improved statistically by the addition of the albedo decay function (Table 3.4); however, the addition of most of the physical parameters generally degrades the ability of the model to predict onset. Graphical analysis suggests that all model variations are able to predict onset adequately, though the algorithms that perform better statistically are also better represented visually (Figure 3.6). Compared to the modified models (Figure 3.6b – 3.6f), BIOME-BGC (v4.2, Figure 3.6a) shows a better graphical relationship with the measured onset date at Stuart Peak.

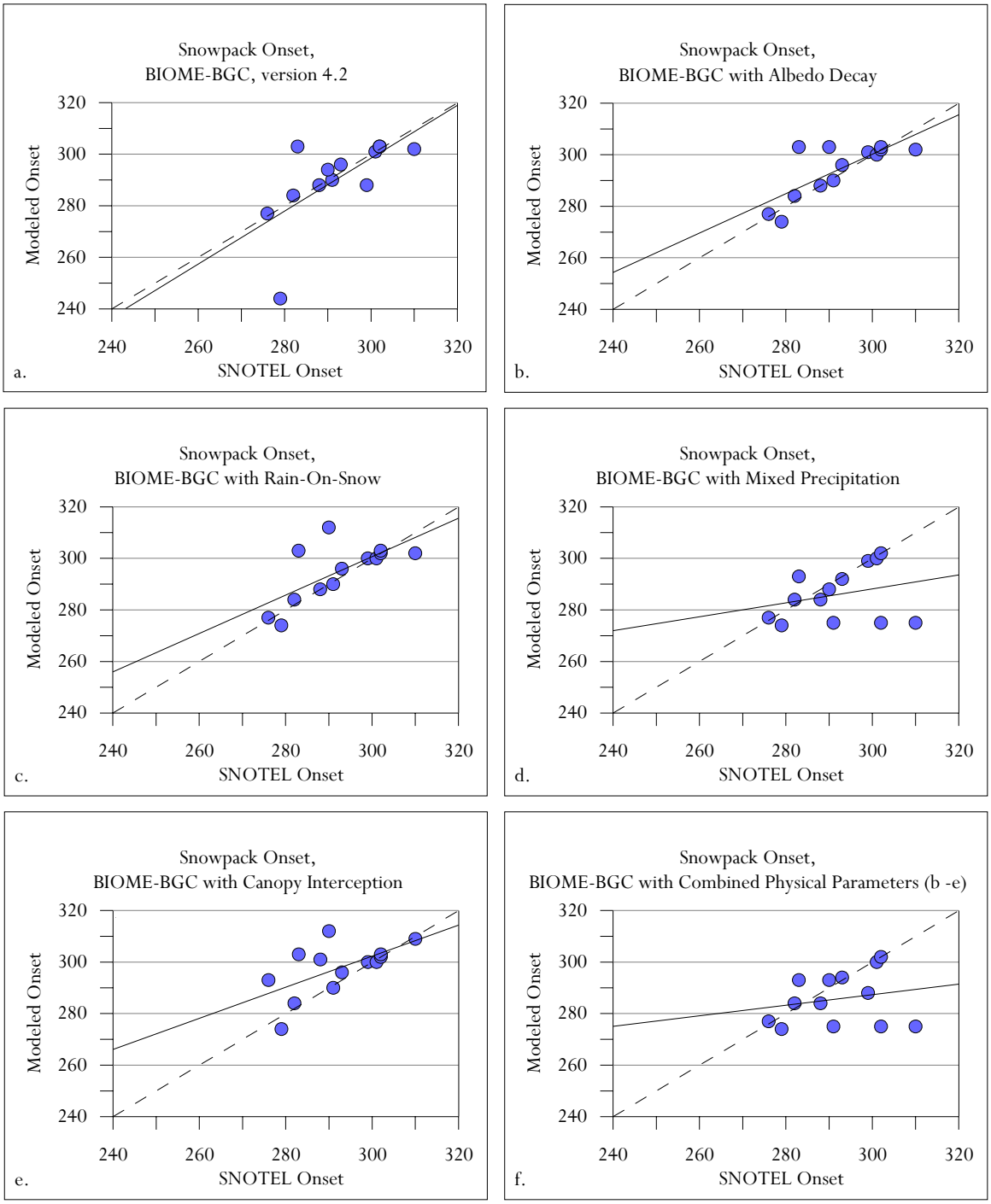

Figure 3.6. Scatterplots comparing the Julian date of measured and modeled snowpack onset at the Stuart Peak SNOTEL. The dashed line represents a one-to-one relationship. The solid line is the regression between the measured and modeled data.

Onset Date	Pred. Mean	Std. Dev.	MAE	RMSE	d	RE (%)	Pearson's r	p
BIOME-BGC v4.2	292.5	10.0	4.4	7.0	0.87	0.2	0.74	<0.5
Albedo Decay	294.1	10.4	4.4	7.2	0.87	0.7	0.76	0.25
Canopy Interception	297.5	10.3	6.7	10.3	0.74	1.9	0.61	0.12
Rain On Snow	294.7	11.3	5.0	8.7	0.82	1.0	0.68	0.29
Mixed	286.0	10.4	8.0	13.5	0.58	-1.8	0.27	0.03
All Parameters	285.7	10.1	8.9	13.8	0.56	-1.9	0.21	0.02

Table 3.4. Validation statistics comparing BIOME-BGC, v4.2 date of snowpack onset at Stuart Peak SNOTEL with several potential physically based model adjustments (n=13). The mean observed date of onset at the Stuart Peak SNOTEL is Julian date 292, with a standard deviation of 10.3.

Most of the individual physical parameters evaluated improve the calculated melt date slightly. Results deteriorate, however, for the mixed precipitation and combined parameter adjustments (Table 3.5). BIOME-BGC and all of the potential physically based changes evaluated here result in an over-prediction of the melt date (Figure 3.7). Most of the physical algorithms evaluated appear to melt the snow-pack earlier than BIOME-BGC (v4.2). Statistically, however, the canopy interception algorithm is the only adjustment that shifts the mean observed melt date so that it is earlier than BIOME-BGC (v4.2; Table 3.5).

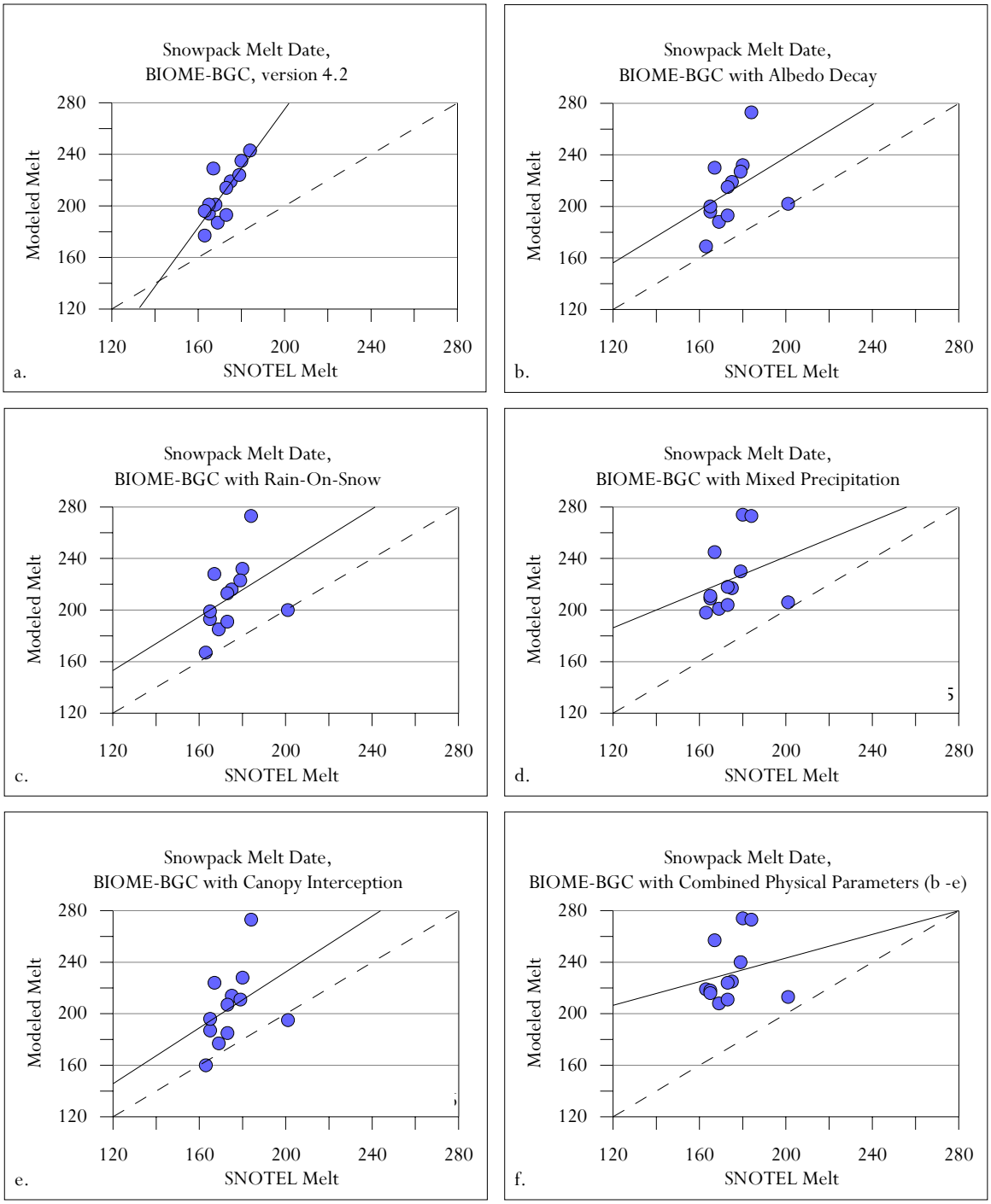

Figure 3.7. Scatterplots comparing the Julian date of the measured and modeled melt date at the Stuart Peak SNOTEL. The dashed line represents a one-to-one relationship. The solid line is the regression between the measured and modeled data.

Melt Date	Predicted Mean	Standard Deviation	MAE	RMSE	d	RE (%)	Pearson's r	p
BIOME-BGC v4.2	208.5	28.0	39.9	44.4	0.22	20.3	0.13	>0.5
Albedo Decay	212.0	27.0	37.5	44.3	0.28	21.5	0.40	<0.5
Canopy Interception	204.8	29.2	31.8	39.7	0.31	17.3	0.40	<0.5
Rain On Snow	210.0	27.5	35.7	42.9	0.29	20.4	0.40	<0.5
Mixed	223.8	26.6	49.3	55.2	0.22	28.4	0.28	<0.5
All Parameters	231.5	23.8	57.0	61.5	0.20	32.9	0.21	<0.5

Table 3.5. Validation statistics comparing BIOME-BGC, v4.2 snowpack melt date at Stuart Peak SNOTEL with several potential physically based model adjustments (n = 12). The mean observed melt Julian date is 173.6, with a standard deviation of 10.7.

Statistical improvements to the modeled snow days are variable (Table 3.6). Again, the addition of the mixed precipitation algorithm and the combined physical parameters generally decrease model efficiency. Inclusion of canopy interception appears to show the best overall statistical improvement over BIOME-BGC (v4.2). All the other parameters tested result in a slight increase, but no method is a beacon of model improvement. Graphically, however, BIOME-BGC (v4.2) appears to outperform all the adjusted models in prediction of snow days (Figure 3.8). All versions of BIOME-BGC consistently over-predict the number of days that snow is present (Figure 3.8, Table 3.6).

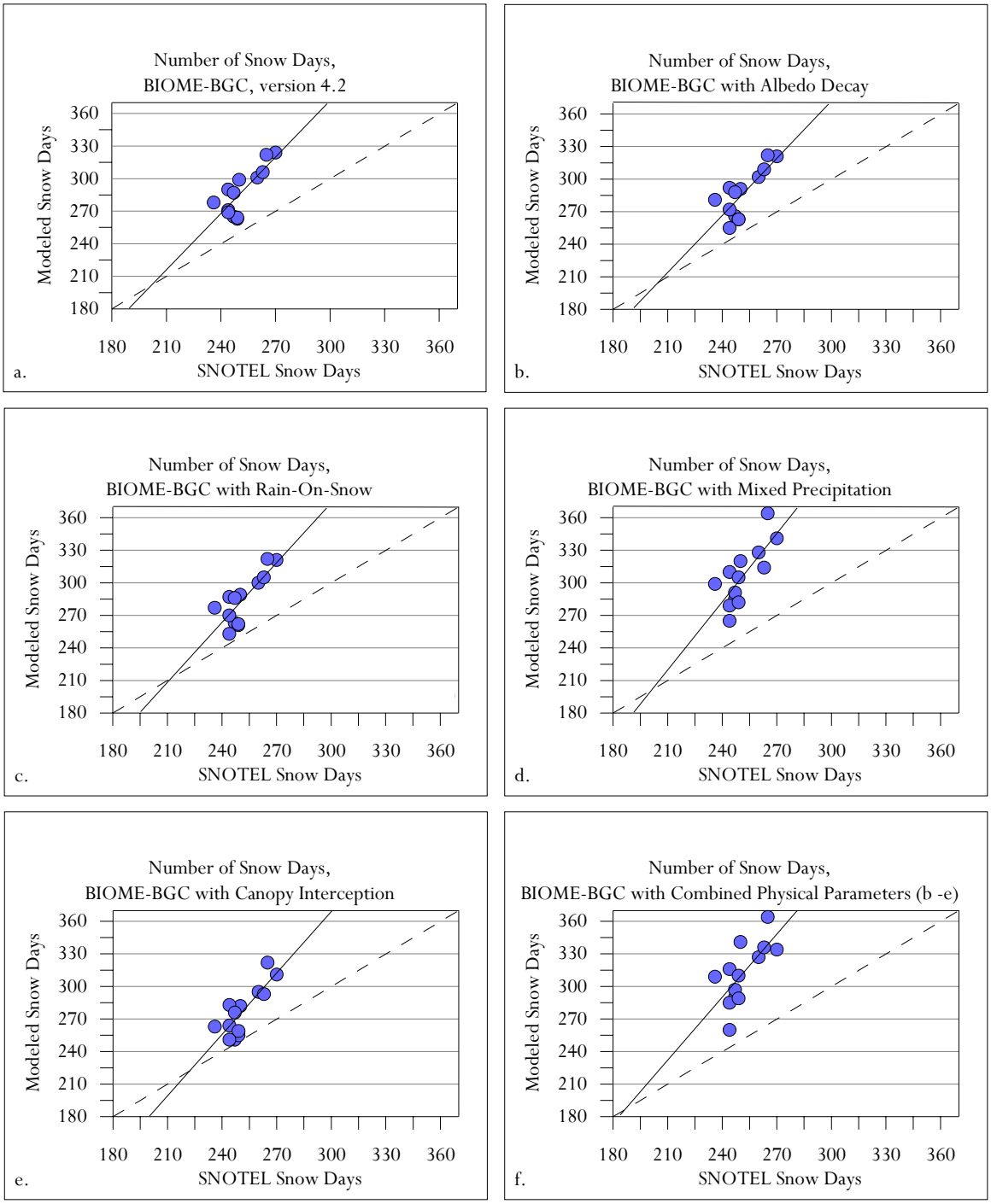

Figure 3.8. Scatterplots comparing the measured and modeled number of days that snow is present at the Stuart Peak SNOTEL. The dashed line represents a one-to-one relationship. The solid line is the regression between the measured and modeled data.

Snow Days	Predicted Mean	Standard Deviation	MAE	RMSE	d	RE (%)	Pearson's r	p
BIOME-BGC v4.2	287.6	21.5	36.2	38.9	0.41	14.3	0.80	<0.5
Albedo	286.5	22.4	35.2	38.3	0.41	13.9	0.78	<0.5
Canopy Interception	277.3	23.0	25.9	30.1	0.50	10.2	0.82	<0.1
Rain On Snow	284.3	22.7	32.9	36.3	0.44	13.0	0.80	<0.5
Mixed	306.4	27.5	55.0	58.6	0.29	21.8	0.76	<0.5
All Parameters	312.2	28.2	60.8	64.5	0.26	24.1	0.68	<0.5

Table 3.6. Validation statistics comparing the days that snow is present at the Stuart Peak SNOTEL as calculated by BIOME-BGC, v4.2 with several potential physically based model adjustments (n=13). The observed mean number of snow days is 251.4, with a standard deviation of 10.0.

3.4 Conclusions

A simple modification to the soil temperature algorithm can significantly improve the ability of the model to predict soil temperature when snow is present. The proposed modification to the snow algorithm presented here lead to mixed results for predicting daily SWE and snowpack evolution. None of the algorithms tested improve model performance enough to warrant addition to current logic; however, future work my find that some combination of the parameters does lead to an improved estimation of SWE and snowpack evolution.

Chapter 4: Proposal of an Accumulated Degree-Day Algorithm in BIOME-BGC

4.1 Introduction

Degree-day snowmelt models are computationally simplistic and utilize easily obtainable meteorological inputs (Hock, 2003). These models have been used in a variety of locations for watersheds of varying size, landscape characteristics and elevation (Ferguson, 1999; WinSRM, 2003), including western Montana (Bleha, 2006).

This chapter conceptualizes and tests potential changes to the degree-day algorithm inherent in the snow-pack subroutine of BIOME-BGC (v4.2). Like chapter 3, the objective here is to adjust the snow model in BIOME-BGC to better predict SWE and snowpack evolution. Model evaluation was performed only on the snow routine, calculated outside the larger BIOME-BGC framework. Again, the cascading effects of the calculations and resulting perturbation to the ecosystem model were not examined by this study.

4.2 Methods

4.2.1 Accumulation and Ablation Degree-Days

The simple degree-day melt algorithm in BIOME-BGC is similar to other models that use a daily temperature index and melt coefficient to calculate snowmelt (Semadeni-Davies, 1997; Westerstrom, 1982). Although this has worked adequately for some models, it appears inadequate at estimating the rate of spring ablation in BIOME-BGC (Section 2.4.3 and 2.4.4). An accumulated degree-day approach, although seldom used in degree-day snowmelt models, may be more appropriate.

Degree-days were accumulated based upon mean daily air temperature, such that,

$$dd_i = (dd_{i-1} + T_{day_i}), \text{ when } T_{day} > 0°C,$$
$$dd_i = (dd_{i-1}), \text{ when } T_{day_i} \leq 0°C, \quad \text{(eq. 4.1)}$$

where dd_i (°C) was the degree day for the present day and dd_{i-1} was the previous day's degree day. Degree days were calculated separately for the accumulation period ($dd_{i,accum}$) and ablation period ($dd_{i,melt}$), but both periods employ the same equation (eq. 4.1). The accumulation period was considered the time between snowpack onset and peak SWE and the ablation period began on the day of peak SWE and lasted until the snowpack was completely melted.

The ablation period degree-day factor (DDF_{melt}) is a coefficient used to calculate daily snowmelt. The DDF_{melt} was parameterized using *in situ* measurements recorded at the Stuart Peak SNOTEL for the ablation period as,

$$DDF_{melt} = melt_i / dd_i. \quad \text{(eq. 4.2)}$$

where $melt_i$ (mm) is the daily snowmelt recorded by the SNOTEL and the DDF_{melt} is the melt coefficient (mm/°C). The annual melt coefficients were then averaged to find the the mean to use in the model.

Modeled snowpack switched from accumulation to ablation after a specified degree-day threshold was met, assumed to be reached at the point of max SWE. The observed max SWE degree-day threshold was calculated using Stuart Peak data, such that

$$dd_{max} = dd_{i,accum} \text{ at peak SWE for year}_j. \quad \text{(eq. 4.3)}$$

Annual calculations of dd_{max} were averaged to parameterize a threshold the model must meet to change into the ablation period. The accumulated degree-day model is also run

using the melt criteria inherent in BIOME-BGC (v4.2) so that melt occurs throughout the snow season whenever $T_{day} > 0°C$.

The average dd_{max} threshold calculated from the Stuart Peak SNOTEL was 83 degree days. The range, however, was large with a low of 12 and a high of 149 (Figure 4.1, Table 4.1). The mean DDF_{melt} calculated for the ablation period was 0.29, with a range of 0.15 – 0.65.

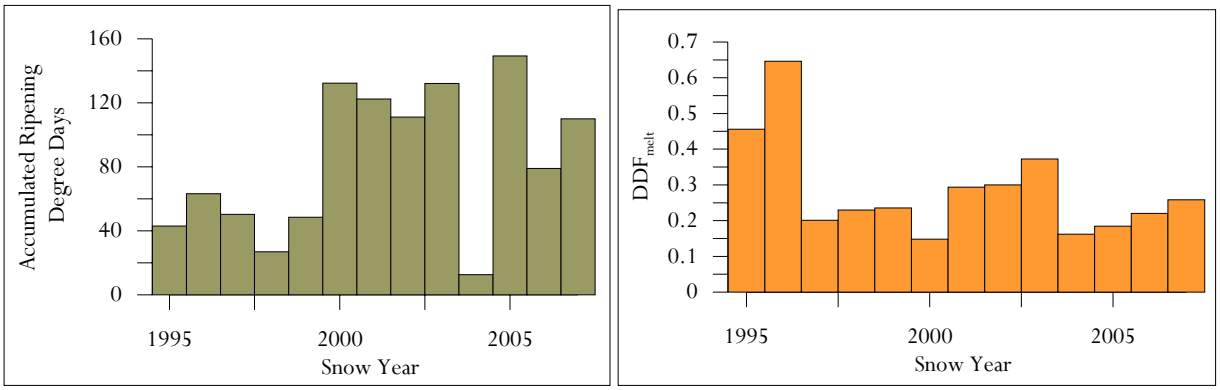

Figure 4.1. Histograms of accumulated dd_{max} and the ablation DDF_{melt} for the period of observation at Stuart Peak SNOTEL, 1996 – 2007.

Snow year	DD_{max}	DDF_{melt}
1995	43	0.46
1996	63	0.65
1997	50	0.20
1998	27	0.23
1999	49	0.24
2000	132	0.15
2001	122	0.29
2002	111	0.30
2003	132	0.37
2004	13	0.16
2005	149	0.18
2006	79	0.22
2007	110	0.26
Mean	83	0.29

Table 4.1 Annual dd_{max} and ablation degree day melt coefficients calculated for the Stuart Peak SNOTEL station.

Sublimation occurs during the accumulation period following the same algorithm used in BIOME-BGC (v4.2; eq. 2.2). Snowmelt was calculated as a linear function of the degree day, such that

$$T_{melt} = dd_{i,melt} * DDF_{melt}. \quad \text{(eq. 4.4)}$$

The algorithm for R_{melt} remains unchanged (eq. 2.4).

4.2.1 Sensitivity Analysis

Using data recorded at an evaluation site to parameterize a model can lead to improved results that will not carry through to other sites. To address this concern, the mean DDF_{melt} calculated from Stuart Peak for the algorithms presented here was adjusted to assess model sensitivity to variance in melt coefficients. Spatial and temporal variability in melt coefficients have been observed in Northwestern Montana (Bleha, 2006). Ablation period melt coefficients calculated for six SNOTEL sites around Northwestern Montana varied around the mean DDF by about 30% (Bleha, 2006).

Model sensitivity to variance in the melt coefficient was tested here by changing the DDF_{melt} by 30% to an upper limit of 0.37 mm/°C and a lower limit of 0.20 mm/°C.

4.2.2 Model Evaluation

Model results were assessed using the Stuart Peak SNOTEL data and will employ the same statistical methods described in Chapter 2 and used in Chapters 2 and 3.

4.3 Results and Discussion

Analysis was done using the existing degree-day method in BIOME-BGC (v4.2) with the newly proposed melt coefficients to parameterize the model. In addition, a version incorporating the proposed accumulated dd_{max} approach was tested with the 3 newly proposed melt coefficients. Results are discussed in relation to daily and peak SWE and snowpack evolution.

4.3.1 Daily and Peak SWE

Graphically, the accumulated degree-day snow-melt algorithm with an ablation period threshold also appears to out perform the model that calculates melt whenever $T_{day} > 0$°C (Figure 4.2). The low melt coefficient shows the best performance for both melt calculations tested here (Figure 4.2b and 4.2e). The accumulated degree-day snow-melt approach with an ablation period threshold far surpasses the snow melt predicted by BIOME-BGC (Figure 4.2a-c and Figure 3.3a). Model error is shifted from over-prediction of daily SWE, as is the case with BIOME-BGC (v4.2; Figure 3.3a & 3.4a), to under-prediction when melt is calculated using accumulated degree days to melt snow

whenever $T_{day} > 0°C$ (Figure 4.2d-e). The time-series graphs support this idea and suggest that all the accumulated degree-day approaches tested here have a problem with under-predicting SWE, especially in the spring (Figure 4.3). Late season under-prediction of SWE is especially pronounced using the degree day approach that calculates melt whenever $T_{day} > 0°C$ (Figure 4.3d-f). All accumulated degree-day algorithms tested here successfully address the problem that BIOME-BGC (v4.2) has with predicting a perennial snowpack for the 1996 snow year (Figure 3.4a and Figure 4.3).

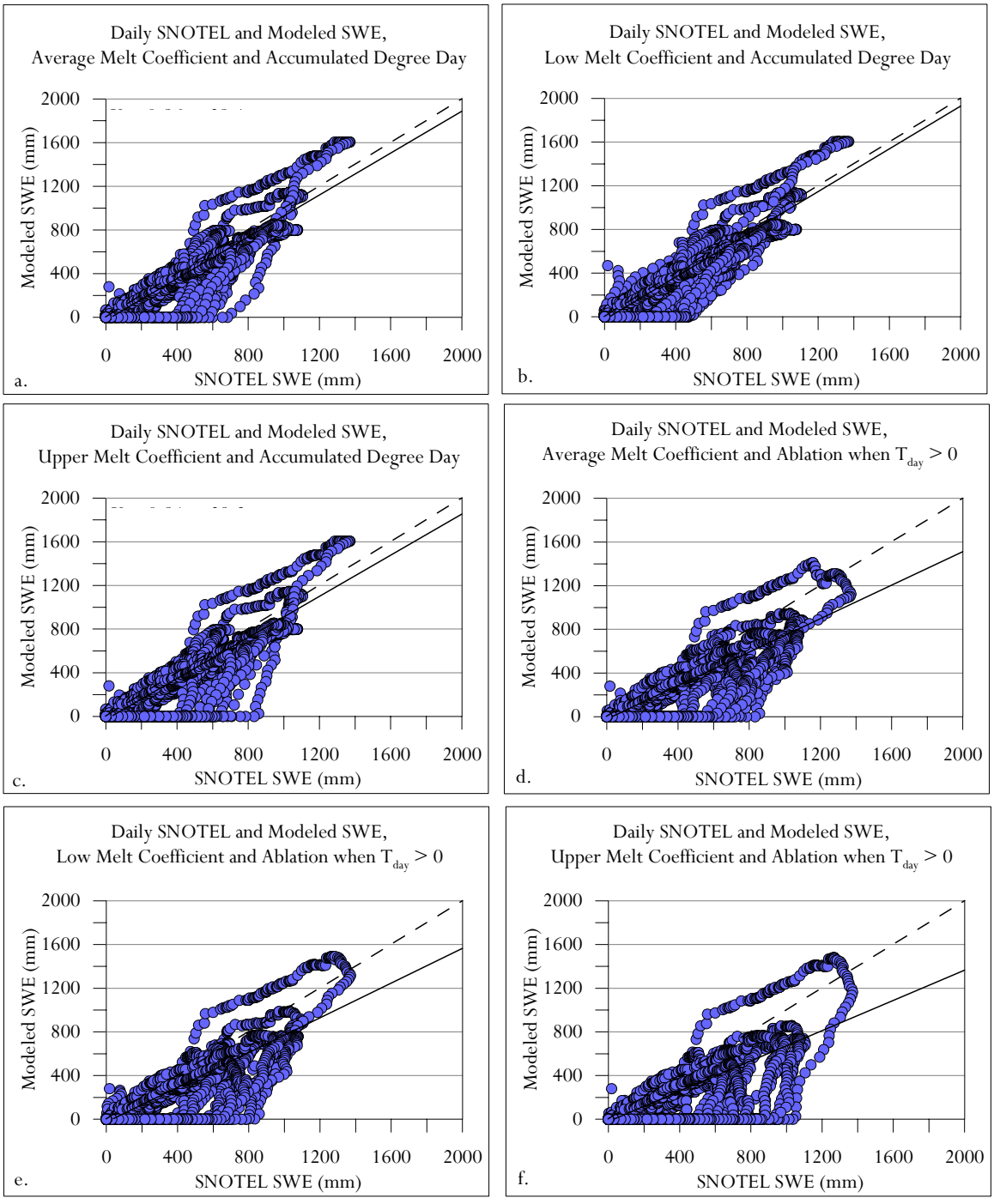

Figure 4.2. Scatterplots of predicted and measured SWE at the Stuart Peak SNOTEL for BIOME-BGC with new degree day algorithms. Figures a-c use an ablation period threshold before calculating melt; Figures d-e calculate melt whenever T_{day} > 0°C. The dashed line represents a one-to-one relationship. The solid line is the linear regression between the predicted and measured SWE.

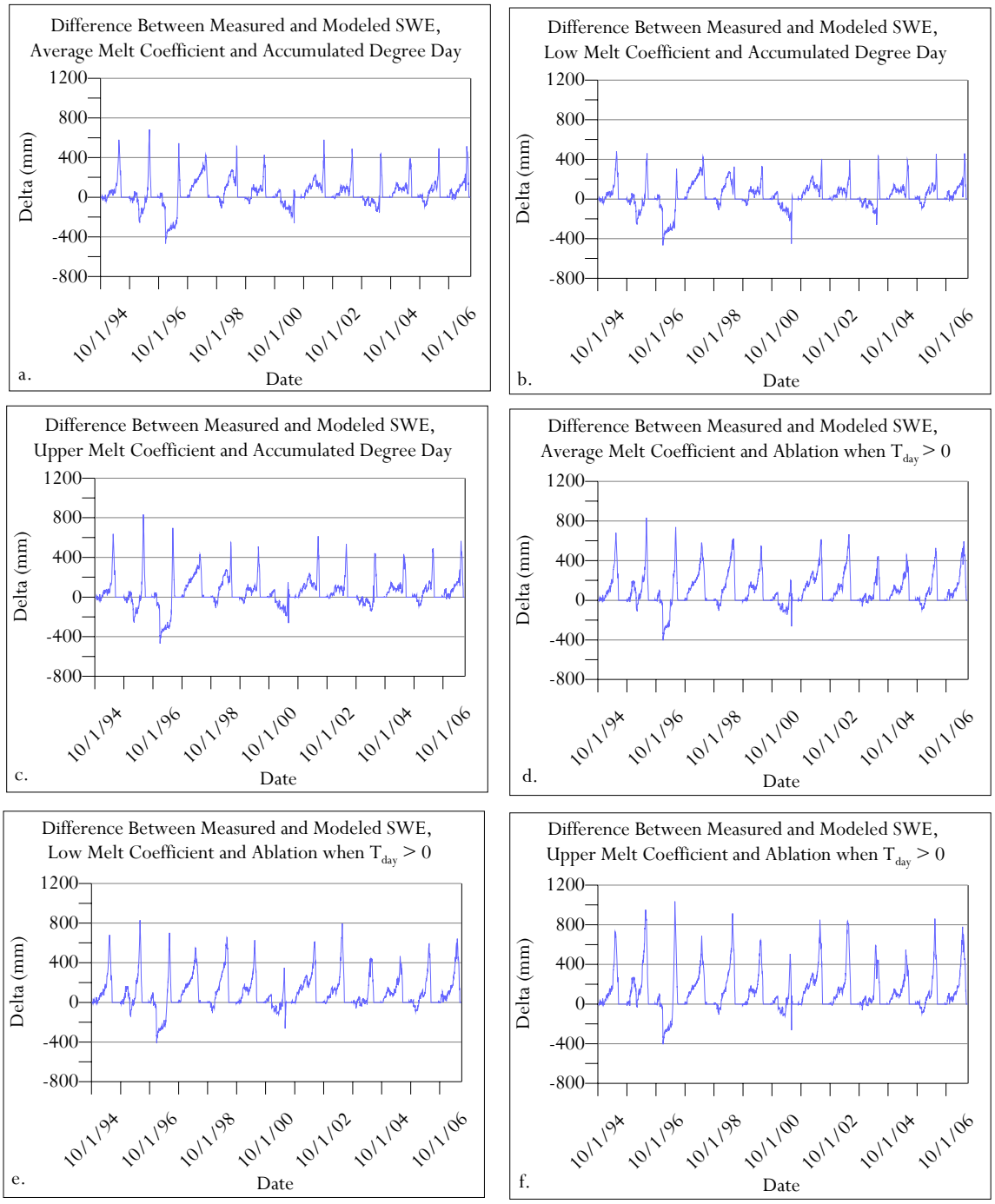

Figure 4.3. Time series graphs illustrating the difference between the measured and modeled daily SWE at the Stuart Peak SNOTEL using BIOME-BGC with new degree-day algorithms. Figures a-c use an ablation period threshold before calculating melt; Figures d-e calculate melt whenever T_{day} > 0°C. Negative values represent model over-prediction; positive values are under-prediction.

Model	Predicted Mean	Standard Deviation	MAE	RMSE	d	RE (%)	Pearson's r	p
BIOME-BGC v4.2	342.0	327.2	113.2	184.9	0.92	56.7	0.85	<0.01
Average DDF, Accumulated dd	286.5	352.3	86.7	139.9	0.96	-15.1	0.93	<0.01
Low DDF, Accumulated dd	295.3	354.8	81.3	126.7	0.97	-11.03	0.94	<0.01
Upper DDF, Accumulated dd	280.8	350.5	91.1	150.8	0.95	-16.4	0.91	<0.01
Average DDF, Ablation when T_{day}>0°C	242.1	316.1	114.8	186.2	0.92	-32.0	0.88	<0.01
Low DDF, Ablation when T_{day}>0°C	235.8	310.7	116.5	191.3	0.91	-32.7	0.87	<0.01
Upper DDF, Ablation when T_{day}>0°C	208.0	293.9	141.3	237.7	0.86	-42.0	0.80	<0.01

Table 4.2. Validation statistics comparing BIOME-BGC, v4.2 daily SWE at Stuart Peak SNOTEL with several degree-day algorithm adjustments (n = 4745). The observed mean for daily SWE at the Stuart Peak SNOTEL is 322.9, with a standard deviation of 340.3.

The accumulated degree-day approach with an ablation period threshold statistically outperforms BIOME-BGC (v4.2) for predicting peak annual SWE (Table 4.3). The accumulated degree-day method that calculates melt whenever T_{day} > 0°C statistically reduces the performance of the model (Table 4.3). Statistically, the model results for calculating peak SWE using the ablation period threshold degree day approach perform equally; however, the low melt coefficient out-performs the average and upper melt coefficient results calculated using the method that melts snow whenever T_{day} > 0°C (Table 4.3). Comparison between the predicted and observed mean peak annual SWE support the idea that all the degree-day methods tested here under-predict SWE.

The idea that adjusting the melt coefficient has little effect on the calculated peak annual SWE for the degree day approach using an ablation period threshold is supported graphically (Figure 4.4 a-c). The graphs, however, do not support the statistical analysis

that the low melt coefficient performs best when melt is calculated for all days that T_{day} > 0°C; graphically, calculating peak SWE using the low melt coefficient results in the worst results (Figure 4.4 d-f). Although all the degree-day methods tested here result in an under-prediction of peak annual SWE, the model using an ablation period threshold appears to be graphically superior to the method that melts snow during T_{day} > 0°C events (Figure 4.4). The slope between measured and modeled peak annual SWE using the accumulated degree day approach that melts snow when T_{day} > 0°C is an improvement over BIOME-BGC (v4.2; Figure 3.5a); however, in general, they do not appear to provide a superior estimation of peak annual SWE. The slope between measured and modeled peak SWE incorporating just the ablation period threshold, on the other hand, is not an improvement over BIOME-BGC (v4.2); however, an overall visual analysis of the graphs suggests similar performance.

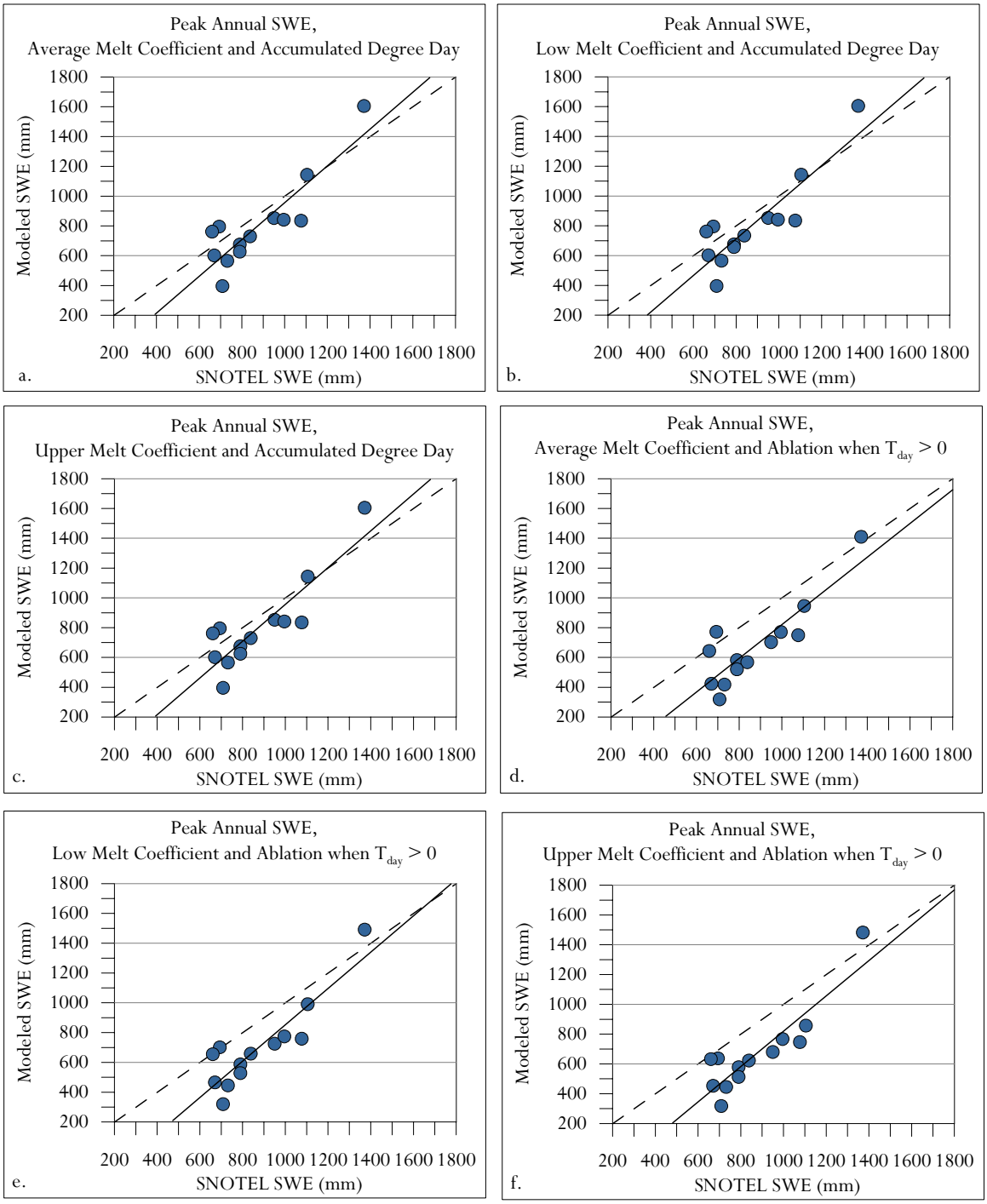

Figure 4.4. Scatterplots of predicted and measured peak annual SWE at the Stuart Peak SNOTEL using BIOME-BGC with new degree-day algorithms. Figures a-c use an ablation period threshold before calculating melt; Figures d-e calculate melt whenever T_{day} > 0°C. The dashed line represents a one-to-one relationship. The solid line is the linear regression between the predicted and measured SWE.

Model	Predicted Mean	Standard Deviation	MAE	RMSE	d	RE (%)	Pearson's r	p
BIOME-BGC v4.2	758.4	289.5	168.6	184.6	0.86	-9.6	0.87	<0.5
Average DDF, Accumulated dd	802.5	300.1	146.2	164.0	0.89	-5.9	0.88	<0.10
Low DDF, Accumulated dd	805.2	298.6	143.5	161.6	0.89	-5.6	0.88	<0.10
Upper DDF, Accumulated dd	802.3	300.2	146.4	164.1	0.89	-6.0	0.88	<0.10
Average DDF, Ablation when T_{day}>0°C	678.9	279.8	214.6	240.6	0.78	-17.2	0.86	<0.01
Low DDF, Ablation when T_{day}>0°C	700.1	293.1	195.0	222.8	0.82	-15.6	0.89	<0.01
Upper DDF, Ablation when T_{day}>0°C	671.9	284.3	220.7	242.0	0.79	-18.8	0.89	<0.01

Table 4.3. Validation statistics comparing peak annual SWE calculated by BIOME-BGC, v4.2 at the Stuart Peak SNOTEL against several potential degree-day adjustments (n=13). The observed mean peak annual SWE at the Stuart Peak SNOTEL is 875.5 with a standard deviation of 213.2.

4.3.2 Snowpack Evolution

The accumulated degree-day algorithm predicts snowpack onset the same regardless of the melt coefficient because no snow is melted until the degree-day threshold is met. All the modifications to the degree-day algorithm tested here degrade the prediction of snowpack onset compared to BIOME-BGC (v4.2; Table 4.4). The mean onset date predicted by BIOME-BGC (v4.2) is in error by only 0.5 days while the modified degree-day algorithms tested result in errors that range between 9 – 14.5 days (Table 4.4).

Graphically, BIOME-BGC (v4.2) shows the best correlation to the measured onset date at Stuart Peak when compared to the modified degree-day algorithms (Figure

4.5 and 3.6a). Some of these modification result in increased error because an accumulated degree-day threshold must be met before any melt can occur (Figure 4.5a). The modifications that allow for snow melt to occur when $T_{day} > 0°C$ likely results in increased error because the accumulated degree days are part of the snowmelt equation (eq. 4.4); not many degree days can accumulate in the early season, resulting in a decrease in early season melt rates compared to BIOME-BGC (v4.2).

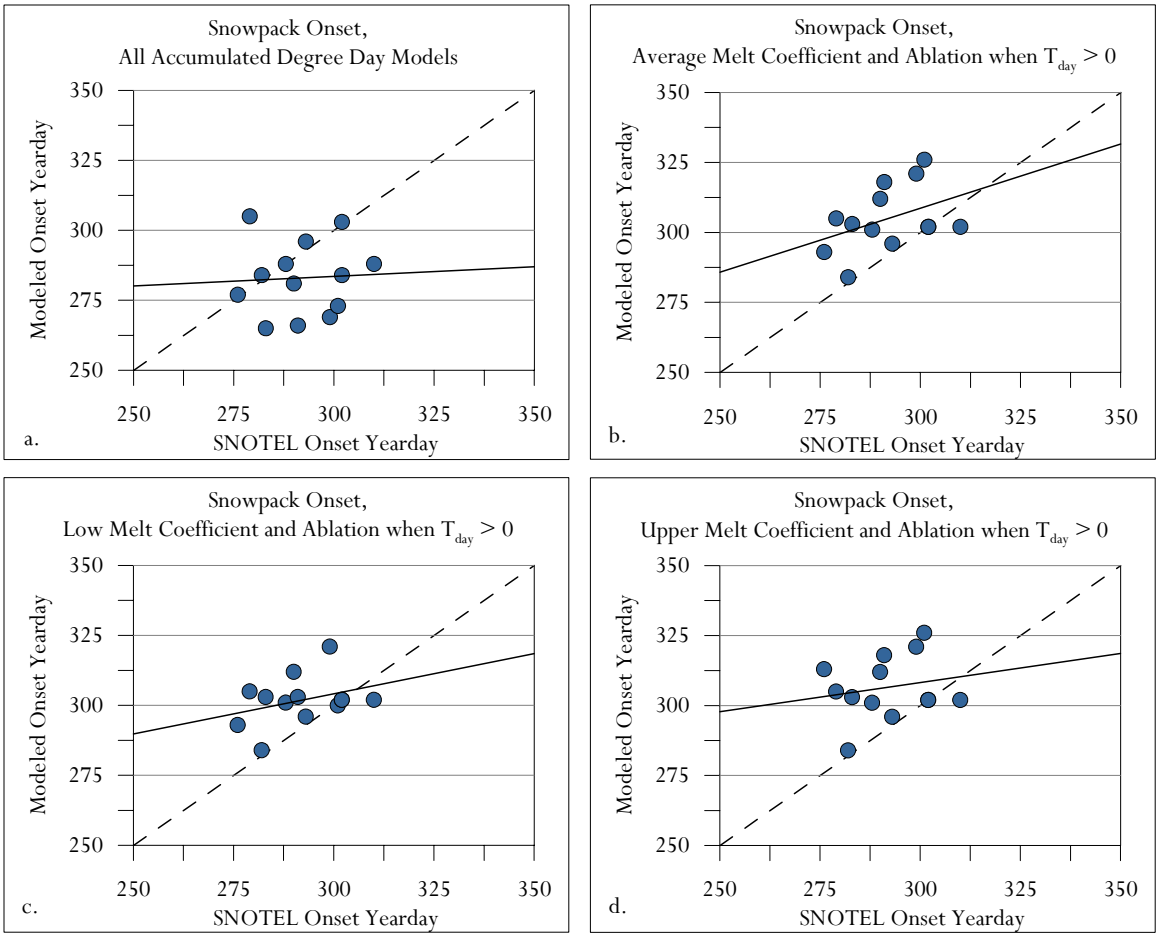

Figure 4.5. Scatterplots comparing the Julian date of measured and modeled snowpack onset at the Stuart Peak SNOTEL. The dashed line represents a one-to-one relationship. The solid line is the regression between the measured and modeled data.

Onset Date	Predicted Mean	Standard Deviation	MAE	RMSE	d	RE (%)	Pearson's r	p
BIOME-BGC v4.2	292.5	10.0	4.4	7.0	0.87	0.2	0.74	<0.5
All Accumulated dd's	283.0	13.1	14.1	18.0	0.41	-3.0	0.05	<0.5
Average DDF, Ablation when T_{day}>0ºC	305.0	11.6	14.2	17.4	0.50	4.5	0.41	<0.01
Low DDF, Ablation when T_{day}>0ºC	301.8	8.7	11.2	14.5	0.52	3.5	0.34	<0.01
Upper DDF, Ablation when T_{day}>0ºC	306.5	11.2	15.8	19.6	0.44	5.1	0.19	<0.01

Table 4.4. Validation statistics comparing the BIOME-BGC, v4.2 date of snowpack onset at Stuart Peak SNOTEL with several potential degree-day model adjustments (n=13). The mean observed date of onset at the Stuart Peak SNOTEL is Julian date 292, with a standard deviation of 10.3.

All the modifications to the degree-day algorithm show statistical improvement over BIOME-BGC (v4.2) with regard to melt date (Table 4.5). The methods that set a degree-day ablation period threshold generally outperform those that calculate melt during T_{day} > 0°C events. Graphical analysis (Figure 4.6 and 3.7a) and examination of the relative error (Table 4.5) suggests that the predicted melt date error has shifted from being too late in BIOME-BGC (v4.2) to too early with all accumulated degree-day modifications. Generally, the predicted melt date using the ablation period threshold with the low DDF_{melt}, although still too early, results in the best performance (Figure 4.6b and Table 4.5). This is likely the result of a slower melt rate due to the smaller melt coefficient.

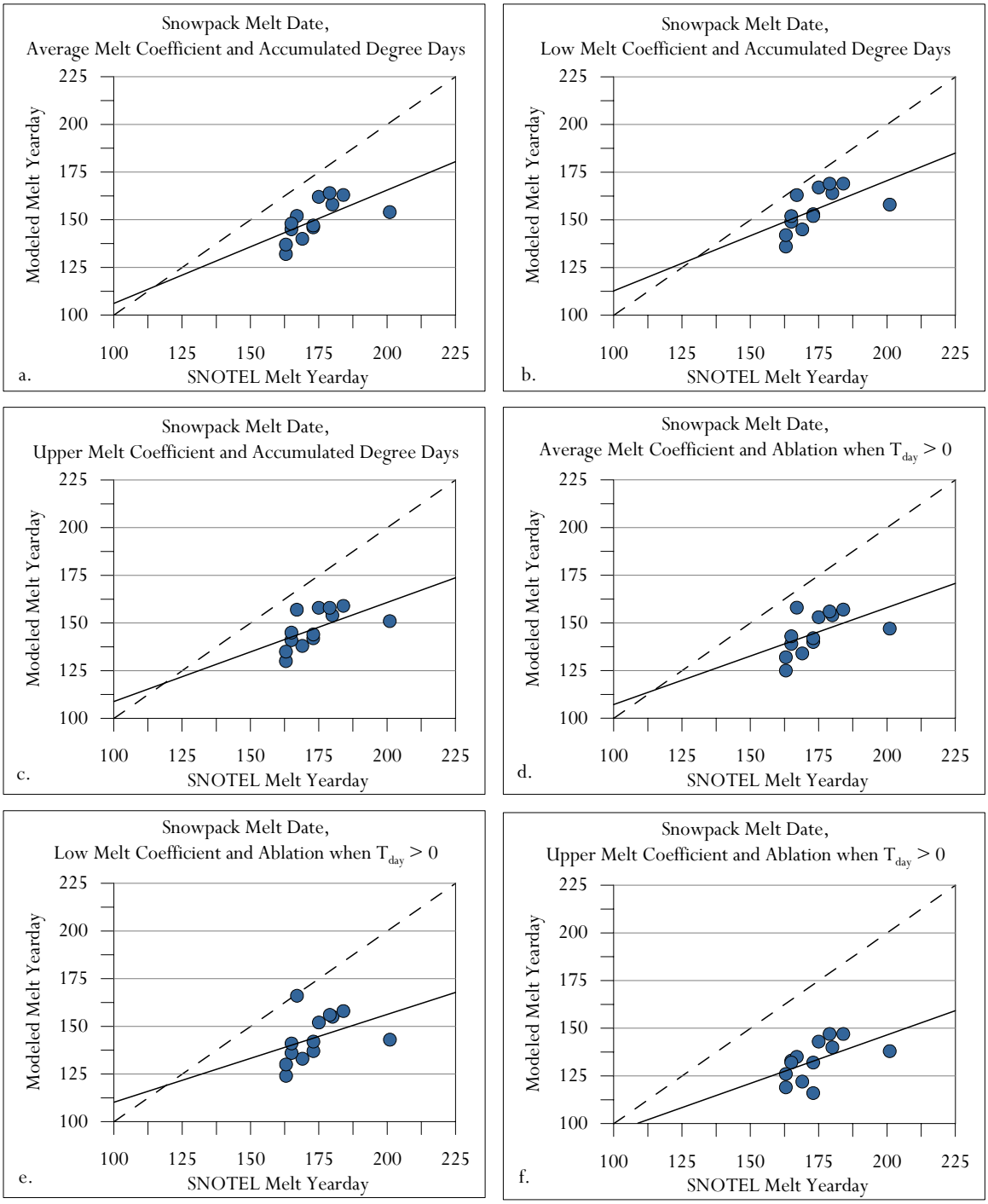

Figure 4.6. Scatter plots comparing the Julian date of the measured and modeled melt date at the Stuart Peak SNOTEL. The dashed line represents a one-to-one relationship. The solid line is the regression between the measured and modeled data.

Melt Date	Predicted Mean	Standard Deviation	MAE	RMSE	d	RE (%)	Pearson's r	p
BIOME-BGC v4.2	208.5	28.0	39.9	44.4	0.22	20.3	0.13	>0.5
Average DDF, Accumulated dd	149.8	10.2	23.8	25.3	0.44	-11.0	0.62	<0.01
Low DDF, Accumulated dd	155.3	10.7	18.3	20.6	0.50	-8.3	0.57	<0.01
Upper DDF, Accumulated dd	147.1	9.7	26.5	28.1	0.40	-12.4	0.57	<0.01
Average DDF, Ablation when T_{day}>0ºC	144.6	10.6	29.0	30.7	0.38	-13.4	0.51	<0.01
Low DDF, Ablation when T_{day}>0ºC	144.1	12.4	29.5	32.0	0.36	-13.6	0.40	<0.01
Upper DDF, Ablation when T_{day}>0ºC	133.1	10.1	40.5	41.7	0.29	-19.0	0.54	<0.01

Table 4.5. Validation statistics comparing BIOME-BGC, v4.2 snowpack melt date at Stuart Peak SNOTEL with several degree-day model adjustments (n = 12). The mean observed melt Julian date is 173.6, with a standard deviation of 10.7.

Examination of the Pearson's r statistic suggests that the accumulated degree-day model that assumes snow melts when T_{day} > 0°C and BIOME-BGC (v4.2) predict the number of snow days with much greater accuracy than the method employing an ablation period degree-day threshold (Table 4.6). However, the MAE, RMSE, RE, and graphs indicate that the ablation period threshold method is superior (Table 4.6, Figure 4.7 and 3.8a). The degree-day approach that melts snow when T_{day} > 0°C grossly under-predicts snow days (Figure 4.7d-f) while BIOME-BGC (v4.2) over-predicts snow days (Figure 3.8a). The accumulated degree-day approach that utilizes an ablation period threshold also results in an overall under-prediction of snow days, however, the relationship between observed and modeled snow days is much closer to one-to-one (Figure 4.7a-c). Again, the low melt coefficient seems to result in the best estimation of snowpack evolution.

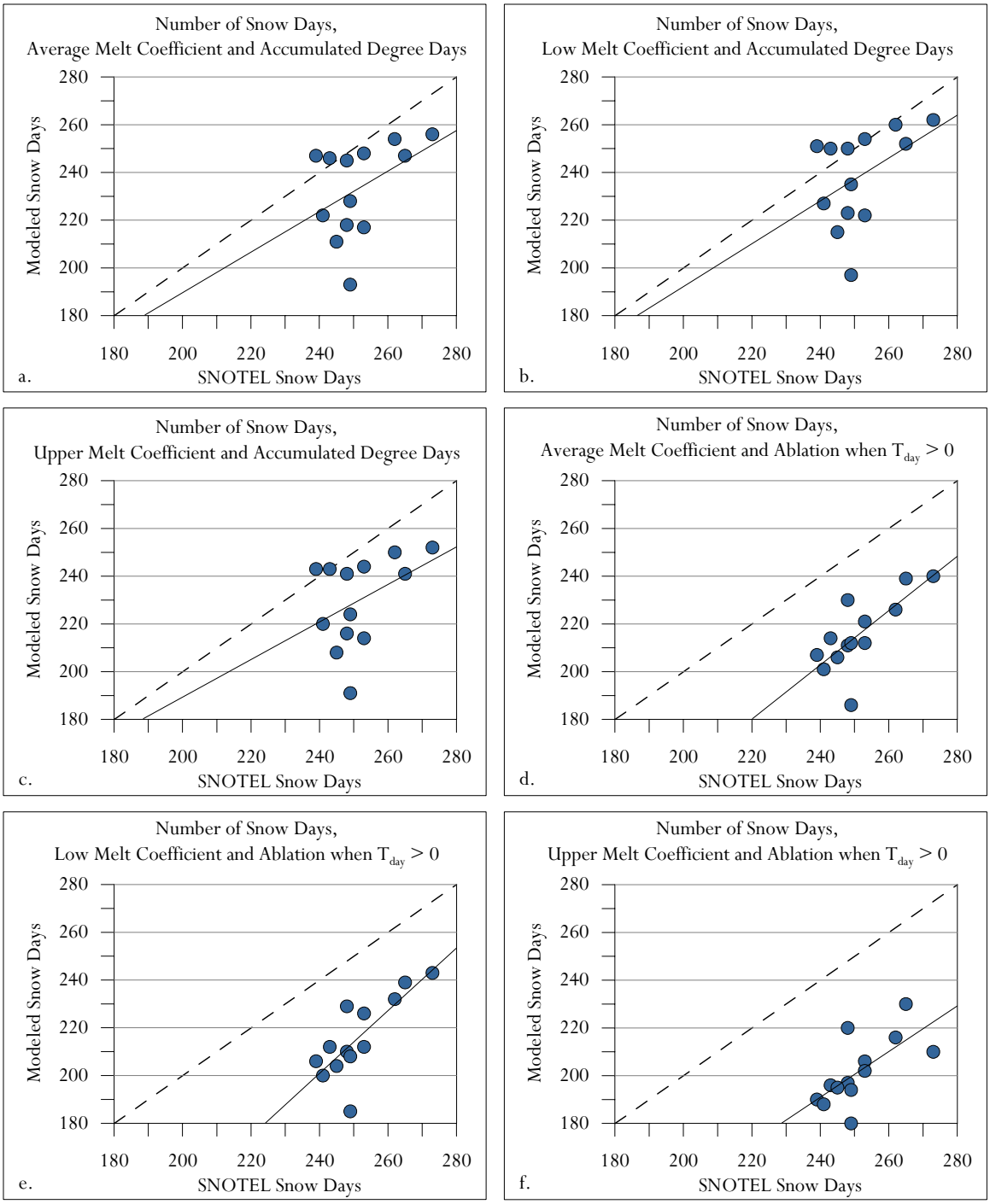

Figure 4.7. Scatterplots comparing the measured and modeled days that snow is present at the Stuart Peak SNOTEL. The dashed line represents a one-to-one relationship. The solid line is the regression between the measured and modeled data.

Snow Days	Predicted Mean	Standard Deviation	MAE	RMSE	d	RE (%)	Pearson's r	p
BIOME-BGC v4.2	287.6	21.5	36.2	38.9	0.41	14.3	0.80	<0.5
Average DDF, Accumulated dd	233.2	19.6	19.8	24.9	0.36	-5.4	0.43	<0.01
Low DDF, Accumulated dd	238.3	20.0	16.5	21.6	0.42	-3.6	0.44	<0.1
Upper DDF, Accumulated dd	229.8	18.8	22.2	27.2	0.32	-6.6	0.41	<0.01
Average DDF, Ablation when T_{day}>0ºC	215.8	15.3	35.6	37.0	0.32	-11.9	0.74	<0.01
Low DDF, Ablation when T_{day}>0ºC	215.8	16.8	35.5	37.1	0.33	-11.8	0.78	<0.01
Upper DDF, Ablation when T_{day}>0ºC	201.8	14.1	49.5	50.5	0.25	-16.6	0.67	<0.01

Table 4.6. Validation statistics comparing the days that snow is present at the Stuart Peak SNOTEL as calculated by BIOME-BGC, v4.2 with several potential degree-day model adjustments (n=13). The observed mean number of snow days is 251.4, with a standard deviation of 10.0.

4.4 Conclusions

Predicted SWE from each of accumulated degree-day algorithms with an ablation period threshold show statistical improvement over BIOME-BGC (v4.2), with the low DDF_{melt} performing best (Table 4.2). BIOME-BGC (v4.2) and the degree-day approach that calculates snowmelt whenever $T_{day} > 0°C$ are statistically similar in SWE estimates for all melt coefficients tested. For both melt criterion tested, the upper melt coefficient was statistically inferior to the average and low melt coefficients. The ability of the low DDF_{melt} to outperform the average DDF_{melt} may be attributed to the use of only one station to parameterize the model.

All modification to the degree-day algorithm tested here degrade the ability of the model to predict snowpack onset. Onset is most negatively effected with the dd_{melt} method because no snow is melted until a threshold is met which causes a persistent snowpack to appear too early in the season. Melt date and snowdays, however, are

improved by nearly all modifications tested here. The most obvious problem with the snow melt algorithm in BIOME-BGC (v4.2) was that all the modifications tested shifted the melt date from too late to too early.

Chapter 5: Conclusions and Recommendations for Future Research

5.1 Lapse Rate

Average temperature lapse rates in the Rattlesnake watershed deviate from the normal lapse rate of -6°C/km for daily maximum temperature and -3°C/km for daily minimum temperature during winter because of temperature inversions and cold air drainage (Table 2.3). Despite the departure from the normal lapse rate, MT-CLIM estimates temperature adequately (Table 2.2) and BIOME-BGC (v4.2) is better able to predict SWE when parameterized with the normal lapse rate. A sensitivity test assessing the response of predicted SWE to different lapse rate parameters in the initialization of BIOME-BGC should be performed if a change to the snow melt algorithm is made in the next version of the model.

5.2 Soil Temperature

The soil temperature algorithms tested here proved more effective than the estimates made by BIOME-BGC (v4.2). However, it may be further improved by using the original calculation proposed by Lagergren et al. (2006) under shallow snowpack and adjusting the decoupling effect of snow to set soil temperature to 0ºC when SWE reaches a certain depth. Taras et al. (2002) found that soil temperature becomes virtually decoupled from air temperature when the snowpack is greater than 80 cm deep. Using a generic 10:1 ratio, this would be about 80 mm of SWE. Future research could test the effectiveness of decoupling soil temperature from air temperature when SWE becomes greater than 80 mm, so that

$$T_{soil} = T_{ra} + (0.2 + (0.8SWE / 5 + SWE))(0.5 - T_{ra}) \text{ when SWE} < 80 \text{ mm}$$

$$T_{soil} = 0 \text{ when SWE} > 80 \text{ mm.} \quad \text{(eq. 5.1)}$$

Restricting the decoupling to times when SWE is greater than 80 mm would have changed the results for both the Rattlesnake Moraine and Woods Gulch site so that the Lagergren algorithm would have been used to estimate soil temperature because SWE remained less than 20mm throughout the winter at both sites (Figure 3.2). Equation 5.1 should be tested for sites where winter snowpack routinely exceeds 80 mm of SWE during the snow year.

5.3 Snowpack

Overall, the accumulated degree-day approach appears to improve model effectiveness better than any of the physical parameters tested in this study. Peak SWE is still under-represented for most years of record and melt dates are consistently calculated too early. This may be improved by including one of the physically based algorithms that increase peak SWE, such as mixed precipitation, in the accumulated degree-day snow-melt subroutine. Several researchers have successfully used this combined partial-energy balance and degree-day approach to simulate annual snowpack development (Kustas et al., 1994; Tague & Band, 2004).

The accumulated degree-day and degree day factor calculations should also be parameterized using several sites throughout the region rather than relying solely on the Stuart Peak SNOTEL. The results of the sensitivity analysis suggest that using several sites to calculate the DDF may result in a lower value melt coefficient. Stuart Peak is a

high elevation site for the region; calculation of the ablation threshold and DDF parameters should include low and mid-elevation sites. Future work employing a degree-day threshold to determine the beginning of the ablation period should also consider the mass of the snow accumulated and the cold content of the snowpack.

It is the opinion of the author that none of the individual parameters improved model efficiency enough to warrant addition to the BIOME-BGC code, except the accumulated degree-day snow-melt approach. The disadvantage of the accumulated degree-day melt algorithm is that it requires users to input regionally optimized values for the degree-day factor and the accumulated degree days required enter the snow ablation period. This should also be tested within the larger framework of BIOME-BGC to assess how it affects the other biophysical components of the model.

The results of this study support the idea that a simple snow-melt algorithm can effectively simulate seasonal SWE, especially when it is part of a larger eco-physical model whose sole purpose is not estimating snowpack characteristics. This study also suggests that the snow model in BIOME-BGC (v4.2) can be improved by expanding it to include some new, still simple, equations. The result of expanding the snow routine in BIOME-BGC (v4.2) may allow future researchers to use model predictions to explore the response of SWE and snowpack evolution to climate perturbations with greater confidence.

Appendix A: MT-CLIM Initialization

	Miss2NE	Rattlesnake Moraine	Woods Gulch	TV Mountain	Stuart Peak
Base elevation, meters	973.00	973.00	973.00	973.00	973.00
Base annual precip isohyet, cm	38.00	38.00	38.00	38.00	38.00
Site latitude, degrees	46.89	46.95	46.92	47.02	46.99
Site elevation, meters	1046.24	1205.49	1491.27	2070.10	2214.90
Site slope, degrees	2.00	15.80	8.40	2.30	2.90
Site aspect, degrees	230.50	217.90	115.90	277.30	150.70
Site annual precip isohyet, cm	48.30	71.10	71.10	116.80	139.70
Site east horizon, degrees	0.00	0.00	33.30	0.00	6.00
Site west horizon, degrees	6.00	42.00	0.00	10.00	0.00
Maximum temperature lapse rate (deg C/ km)	-6.00	-6.00	-6.00	-6.00	-6.00
Minimum temperature lapse rate (deg C/ km)	-3.00	-3.00	-3.00	-3.00	-3.00

Appendix B: BIOME-BGC Initialization Files

Miss2NE

```
TIME_DEFINE   (keyword - do not remove)
58          (int)      number of meteorological data years
58          (int)      number of simulation years
1950        (int)      first simulation year
0           (flag)     1 = spinup simulation    0 = normal simulation
6000        (int)      maximum number of spinup years (if spinup simulation)

CLIM_CHANGE   (keyword - do not remove)
0.0         (deg C)   offset for Tmax
0.0         (deg C)   offset for Tmin
1.0         (DIM)     multiplier for Prcp
1.0         (DIM)     multiplier for VPD
1.0         (DIM)     multiplier for shortwave radiation

CO2_CONTROL   (keyword - do not remove)
1           (flag)    0=constant 1=vary with file 2=constant, file for Ndep
311.172     (ppm)     constant atmospheric CO2 concentration
co2/co2.txt   (file)    annual variable CO2 filename

DISTURBANCE_CONTROL        (keyword - do not remove)
0               (int) number of disturbances

SITE         (keyword) start of site physical constants block
1.0         (m)       effective soil depth (corrected for rock fraction)
43.8        (%)       sand percentage by volume in rock-free soil
40.2        (%)       silt percentage by volume in rock-free soil
16.0        (%)       clay percentage by volume in rock-free soil
1046.24     (m)       site elevation
46.89       (degrees) site latitude (- for S.Hem.)
0.17        (DIM)     site shortwave albedo
0.0001      (kgN/m2/yr) wet+dry atmospheric deposition of N
0.0004      (kgN/m2/yr) symbiotic+asymbiotic fixation of N

RAMP_NDEP     (keyword - do not remove)
0           (flag) do a ramped N-deposition run? 0=no, 1=yes
2099        (int)  reference year for industrial N deposition
0.0001      (kgN/m2/yr) industrial N deposition value

EPC_FILE      (keyword - do not remove)
epc/c3grass.epc   (file) grass ecophysiological constants

W_STATE       (keyword) start of water state variable initialization block
0.0         (kg/m2)   water stored in snowpack
0.5         (DIM)     initial soil water as a proportion of saturation

C_STATE       (keyword) start of carbon state variable initialization block
0.001       (kgC/m2)  first-year maximum leaf carbon
0.0         (kgC/m2)  first-year maximum stem carbon
0.0         (kgC/m2)  coarse woody debris carbon
0.0         (kgC/m2)  litter carbon, labile pool
0.0         (kgC/m2)  litter carbon, unshielded cellulose pool
```

```
0.0         (kgC/m2)  litter carbon, shielded cellulose pool
0.0         (kgC/m2)  litter carbon, lignin pool
0.0         (kgC/m2)  soil carbon, fast microbial recycling pool
0.0         (kgC/m2)  soil carbon, medium microbial recycling pool
0.0         (kgC/m2)  soil carbon, slow microbial recycling pool
0.0         (kgC/m2)  soil carbon, recalcitrant SOM (slowest)

N_STATE      (keyword) start of nitrogen state variable initialization block
0.0         (kgN/m2)  litter nitrogen, labile pool
0.0         (kgN/m2)  soil nitrogen, mineral pool

OUTPUT_CONTROL   (keyword - do not remove)
outputs/grass_miss2ne_5007     (text) prefix for output files
1   (flag)  1 = write daily output   0 = no daily output
0   (flag)  1 = monthly avg of daily variables  0 = no monthly avg
0   (flag)  1 = annual avg of daily variables   0 = no annual avg
1  (flag)  1 = write annual output  0 = no annual output
1   (flag)  1 = write disturbance text output  0 = no disturbance output
1   (flag)  for on-screen progress indicator

DAILY_OUTPUT     (keyword)
17    (int) number of daily variables to output
0          0 metv.prcp (kg/m2)
1          1 metv.tmax (deg C)
2          2 metv.tmin (deg C)
6          3 metv.tsoil (deg C)
20         4 ws.soilw (kgH2O/m2)
21         5 ws.snoww (kgH2O/m2)
22         6 ws.canopyw (kgH2O/m2)
24         7 ws.outflow_snk (kgH2O/m2)
25         8 ws.soilevap_snk (kgH2O/m2)
26         9 ws.snowsubl_snk (kgH2O/m2)
35         10 wf.prcp_to_canopyw (kgH2O/m2/d)
36         11 wf.prcp_to_soilw (kgH2O/m2/d)
37         12 wf.prcp_to_snow (kgH2O/m2/d)
40         13 wf.snoww_subl (kgH2O/m2/d)
41         14 wf.snoww_to_soilw (kgH2O/m2/d)
42         15 wf.soilw_evap (kgH2O/m2/d)
44         16 wf.soilw_outflow (kgH2O/m2/d)

ANNUAL_OUTPUT    (keyword)
4             (int)   number of annual output variables
21         1 ws.snoww (kgH2O/m2)
26         2 ws.snowsubl_snk (kgH2O/m2)
20         3 ws.soilw (kgH2O/m2)
21         4 ws.snoww (kgH2O/m2)
```

Rattlesnake Moraine

```
TIME_DEFINE   (keyword - do not remove)
58          (int)      number of meteorological data years
58          (int)      number of simulation years
1950         (int)      first simulation year
0           (flag)     1 = spinup simulation    0 = normal simulation
6000         (int)      maximum number of spinup years (if spinup simulation)
```

```
CLIM_CHANGE   (keyword - do not remove)
0.0         (deg C)   offset for Tmax
0.0         (deg C)   offset for Tmin
1.0         (DIM)     multiplier for Prcp
1.0         (DIM)     multiplier for VPD
1.0         (DIM)     multiplier for shortwave radiation

CO2_CONTROL   (keyword - do not remove)
1           (flag)    0=constant 1=vary with file 2=constant, file for Ndep
311.172       (ppm)     constant atmospheric CO2 concentration
co2/co2.txt   (file)    annual variable CO2 filename

DISTURBANCE_CONTROL        (keyword - do not remove)
0               (int)  number of disturbances

SITE         (keyword) start of site physical constants block
1.0          (m)       effective soil depth (corrected for rock fraction)
45           (%)       sand percentage by volume in rock-free soil
41.5         (%)       silt percentage by volume in rock-free soil
13.5         (%)       clay percentage by volume in rock-free soil
1205.49      (m)       site elevation
46.95        (degrees) site latitude (- for S.Hem.)
0.17         (DIM)     site shortwave albedo
0.0001       (kgN/m2/yr) wet+dry atmospheric deposition of N
0.0004       (kgN/m2/yr) symbiotic+asymbiotic fixation of N

RAMP_NDEP     (keyword - do not remove)
0           (flag) do a ramped N-deposition run? 0=no, 1=yes
2099         (int)  reference year for industrial N deposition
0.0001       (kgN/m2/yr) industrial N deposition value

EPC_FILE      (keyword - do not remove)
epc/enf.epc   (file) evergreen needleleaf forest ecophysiological constants

W_STATE       (keyword) start of water state variable initialization block
0.0          (kg/m2)   water stored in snowpack
0.5          (DIM)     initial soil water as a proportion of saturation

C_STATE       (keyword) start of carbon state variable initialization block
0.001        (kgC/m2)  first-year maximum leaf carbon
0.0          (kgC/m2)  first-year maximum stem carbon
0.0          (kgC/m2)  coarse woody debris carbon
0.0          (kgC/m2)  litter carbon, labile pool
0.0          (kgC/m2)  litter carbon, unshielded cellulose pool
0.0          (kgC/m2)  litter carbon, shielded cellulose pool
0.0          (kgC/m2)  litter carbon, lignin pool
0.0          (kgC/m2)  soil carbon, fast microbial recycling pool
0.0          (kgC/m2)  soil carbon, medium microbial recycling pool
0.0          (kgC/m2)  soil carbon, slow microbial recycling pool
0.0          (kgC/m2)  soil carbon, recalcitrant SOM (slowest)

N_STATE       (keyword) start of nitrogen state variable initialization block
0.0          (kgN/m2)  litter nitrogen, labile pool
0.0          (kgN/m2)  soil nitrogen, mineral pool

OUTPUT_CONTROL   (keyword - do not remove)
```

```
outputs/rattlesnake_5007     (text) prefix for output files
1   (flag)  1 = write daily output   0 = no daily output
0   (flag)  1 = monthly avg of daily variables  0 = no monthly avg
0   (flag)  1 = annual avg of daily variables   0 = no annual avg
1  (flag)  1 = write annual output  0 = no annual output
1   (flag)  1 = write disturbance text output  0 = no disturbance output
1   (flag)  for on-screen progress indicator

DAILY_OUTPUT     (keyword)
17    (int) number of daily variables to output
0          0 metv.prcp (kg/m2)
1          1 metv.tmax (deg C)
2          2 metv.tmin (deg C)
6          3 metv.tsoil (deg C)
20         4 ws.soilw (kgH2O/m2)
21         5 ws.snoww (kgH2O/m2)
22         6 ws.canopyw (kgH2O/m2)
24         7 ws.outflow_snk (kgH2O/m2)
25         8 ws.soilevap_snk (kgH2O/m2)
26         9 ws.snowsubl_snk (kgH2O/m2)
35         10 wf.prcp_to_canopyw (kgH2O/m2/d)
36         11 wf.prcp_to_soilw (kgH2O/m2/d)
37         12 wf.prcp_to_snow (kgH2O/m2/d)
40         13 wf.snoww_subl (kgH2O/m2/d)
41         14 wf.snoww_to_soilw (kgH2O/m2/d)
42         15 wf.soilw_evap (kgH2O/m2/d)
44         16 wf.soilw_outflow (kgH2O/m2/d)

ANNUAL_OUTPUT    (keyword)
4             (int)   number of annual output variables
21         1 ws.snoww (kgH2O/m2)
26         2 ws.snowsubl_snk (kgH2O/m2)
20         3 ws.soilw (kgH2O/m2)
21         4 ws.snoww (kgH2O/m2)
```

Woods Gulch

```
TIME_DEFINE   (keyword - do not remove)
58          (int)      number of meteorological data years
58          (int)      number of simulation years
1950         (int)      first simulation year
0           (flag)     1 = spinup simulation    0 = normal simulation
6000         (int)      maximum number of spinup years (if spinup simulation)

CLIM_CHANGE   (keyword - do not remove)
0.0         (deg C)   offset for Tmax
0.0         (deg C)   offset for Tmin
1.0         (DIM)     multiplier for Prcp
1.0         (DIM)     multiplier for VPD
1.0         (DIM)     multiplier for shortwave radiation

CO2_CONTROL   (keyword - do not remove)
1           (flag)    0=constant 1=vary with file 2=constant, file for Ndep
311.172       (ppm)     constant atmospheric CO2 concentration
co2/co2.txt   (file)    annual variable CO2 filename
```

```
DISTURBANCE_CONTROL        (keyword - do not remove)
0                (int)  number of disturbances

SITE         (keyword) start of site physical constants block
1.0          (m)       effective soil depth (corrected for rock fraction)
45.7         (%)       sand percentage by volume in rock-free soil
41.8         (%)       silt percentage by volume in rock-free soil
12.5         (%)       clay percentage by volume in rock-free soil
1491.27      (m)       site elevation
46.92        (degrees) site latitude (- for S.Hem.)
0.17         (DIM)     site shortwave albedo
0.0001       (kgN/m2/yr) wet+dry atmospheric deposition of N
0.0004       (kgN/m2/yr) symbiotic+asymbiotic fixation of N

RAMP_NDEP     (keyword - do not remove)
0           (flag) do a ramped N-deposition run? 0=no, 1=yes
2099         (int)  reference year for industrial N deposition
0.0001       (kgN/m2/yr) industrial N deposition value

EPC_FILE      (keyword - do not remove)
epc/enf.epc   (file) evergreen needleleaf forest ecophysiological constants

W_STATE       (keyword) start of water state variable initialization block
0.0          (kg/m2)   water stored in snowpack
0.5          (DIM)     initial soil water as a proportion of saturation

C_STATE       (keyword) start of carbon state variable initialization block
0.001        (kgC/m2)  first-year maximum leaf carbon
0.0          (kgC/m2)  first-year maximum stem carbon
0.0          (kgC/m2)  coarse woody debris carbon
0.0          (kgC/m2)  litter carbon, labile pool
0.0          (kgC/m2)  litter carbon, unshielded cellulose pool
0.0          (kgC/m2)  litter carbon, shielded cellulose pool
0.0          (kgC/m2)  litter carbon, lignin pool
0.0          (kgC/m2)  soil carbon, fast microbial recycling pool
0.0          (kgC/m2)  soil carbon, medium microbial recycling pool
0.0          (kgC/m2)  soil carbon, slow microbial recycling pool
0.0          (kgC/m2)  soil carbon, recalcitrant SOM (slowest)

N_STATE       (keyword) start of nitrogen state variable initialization block
0.0          (kgN/m2)  litter nitrogen, labile pool
0.0          (kgN/m2)  soil nitrogen, mineral pool

OUTPUT_CONTROL   (keyword - do not remove)
outputs/woodsgulch_5007     (text) prefix for output files
1   (flag)  1 = write daily output   0 = no daily output
0   (flag)  1 = monthly avg of daily variables  0 = no monthly avg
0   (flag)  1 = annual avg of daily variables   0 = no annual avg
1  (flag)  1 = write annual output  0 = no annual output
1   (flag)  1 = write disturbance text output  0 = no disturbance output
1   (flag)  for on-screen progress indicator

DAILY_OUTPUT     (keyword)
17     (int) number of daily variables to output
0           0 metv.prcp (kg/m2)
1           1 metv.tmax (deg C)
```

```
2          2 metv.tmin (deg C)
6          3 metv.tsoil (deg C)
20         4 ws.soilw (kgH2O/m2)
21         5 ws.snoww (kgH2O/m2)
22         6 ws.canopyw (kgH2O/m2)
24         7 ws.outflow_snk (kgH2O/m2)
25         8 ws.soilevap_snk (kgH2O/m2)
26         9 ws.snowsubl_snk (kgH2O/m2)
35         10 wf.prcp_to_canopyw (kgH2O/m2/d)
36         11 wf.prcp_to_soilw (kgH2O/m2/d)
37         12 wf.prcp_to_snow (kgH2O/m2/d)
40         13 wf.snoww_subl (kgH2O/m2/d)
41         14 wf.snoww_to_soilw (kgH2O/m2/d)
42         15 wf.soilw_evap (kgH2O/m2/d)
44         16 wf.soilw_outflow (kgH2O/m2/d)

ANNUAL_OUTPUT    (keyword)
4            (int)   number of annual output variables
21         1 ws.snoww (kgH2O/m2)
26         2 ws.snowsubl_snk (kgH2O/m2)
20         3 ws.soilw (kgH2O/m2)
21         4 ws.snoww (kgH2O/m2)
```

TV Mountain

```
TIME_DEFINE   (keyword - do not remove)
58          (int)      number of meteorological data years
58          (int)      number of simulation years
1950         (int)      first simulation year
0           (flag)     1 = spinup simulation    0 = normal simulation
6000         (int)      maximum number of spinup years (if spinup simulation)

CLIM_CHANGE   (keyword - do not remove)
0.0         (deg C)   offset for Tmax
0.0         (deg C)   offset for Tmin
1.0         (DIM)     multiplier for Prcp
1.0         (DIM)     multiplier for VPD
1.0         (DIM)     multiplier for shortwave radiation

CO2_CONTROL   (keyword - do not remove)
1           (flag)    0=constant 1=vary with file 2=constant, file for Ndep
311.172       (ppm)     constant atmospheric CO2 concentration
co2/co2.txt   (file)    annual variable CO2 filename

DISTURBANCE_CONTROL        (keyword - do not remove)
0               (int) number of disturbances

SITE         (keyword) start of site physical constants block
1.0         (m)       effective soil depth (corrected for rock fraction)
45.0         (%)       sand percentage by volume in rock-free soil
45.0         (%)       silt percentage by volume in rock-free soil
10.0         (%)       clay percentage by volume in rock-free soil
2070.1       (m)       site elevation
47.01944      (degrees) site latitude (- for S.Hem.)
0.17         (DIM)     site shortwave albedo
0.0004       (kgN/m2/yr) wet+dry atmospheric deposition of N
```

```
0.0004       (kgN/m2/yr) symbiotic+asymbiotic fixation of N

RAMP_NDEP     (keyword - do not remove)
0           (flag) do a ramped N-deposition run? 0=no, 1=yes
2099         (int)  reference year for industrial N deposition
0.0001       (kgN/m2/yr) industrial N deposition value

EPC_FILE      (keyword - do not remove)
epc/enf.epc   (file) evergreen needleleaf forest ecophysiological constants

W_STATE       (keyword) start of water state variable initialization block
0.0          (kg/m2)   water stored in snowpack
0.5          (DIM)     initial soil water as a proportion of saturation

C_STATE       (keyword) start of carbon state variable initialization block
0.001         (kgC/m2)  first-year maximum leaf carbon
0.0          (kgC/m2)  first-year maximum stem carbon
0.0          (kgC/m2)  coarse woody debris carbon
0.0          (kgC/m2)  litter carbon, labile pool
0.0          (kgC/m2)  litter carbon, unshielded cellulose pool
0.0          (kgC/m2)  litter carbon, shielded cellulose pool
0.0          (kgC/m2)  litter carbon, lignin pool
0.0          (kgC/m2)  soil carbon, fast microbial recycling pool
0.0          (kgC/m2)  soil carbon, medium microbial recycling pool
0.0          (kgC/m2)  soil carbon, slow microbial recycling pool
0.0          (kgC/m2)  soil carbon, recalcitrant SOM (slowest)

N_STATE       (keyword) start of nitrogen state variable initialization block
0.0          (kgN/m2)  litter nitrogen, labile pool
0.0          (kgN/m2)  soil nitrogen, mineral pool

OUTPUT_CONTROL   (keyword - do not remove)
outputs/tvmt_5007     (text) prefix for output files
1   (flag)  1 = write daily output   0 = no daily output
0   (flag)  1 = monthly avg of daily variables  0 = no monthly avg
0   (flag)  1 = annual avg of daily variables   0 = no annual avg
1   (flag)  1 = write annual output  0 = no annual output
1   (flag)  1 = write disturbance text output  0 = no disturbance output
1   (flag)  for on-screen progress indicator

DAILY_OUTPUT     (keyword)
17      (int) number of daily variables to output
0            0 metv.prcp (kg/m2)
1            1 metv.tmax (deg C)
2            2 metv.tmin (deg C)
6            3 metv.tsoil (deg C)
20           4 ws.soilw (kgH2O/m2)
21           5 ws.snoww (kgH2O/m2)
22           6 ws.canopyw (kgH2O/m2)
24           7 ws.outflow_snk (kgH2O/m2)
25           8 ws.soilevap_snk (kgH2O/m2)
26           9 ws.snowsubl_snk (kgH2O/m2)
35           10 wf.prcp_to_canopyw (kgH2O/m2/d)
36           11 wf.prcp_to_soilw (kgH2O/m2/d)
37           12 wf.prcp_to_snow (kgH2O/m2/d)
40           13 wf.snoww_subl (kgH2O/m2/d)
```

```
41          14 wf.snoww_to_soilw (kgH2O/m2/d)
42          15 wf.soilw_evap (kgH2O/m2/d)
44          16 wf.soilw_outflow (kgH2O/m2/d)

ANNUAL_OUTPUT    (keyword)
4      (int)   number of annual output variables
21          0 ws.snoww (kgH2O/m2)
26          1 ws.snowsubl_snk (kgH2O/m2)
20          2 ws.soilw (kgH2O/m2)
21          3 ws.snoww (kgH2O/m2)
```

Stuart Peak

```
TIME_DEFINE   (keyword - do not remove)
58          (int)       number of meteorological data years
58          (int)       number of simulation years
1950          (int)       first simulation year
0           (flag)      1 = spinup simulation    0 = normal simulation
6000          (int)       maximum number of spinup years (if spinup simulation)

CLIM_CHANGE   (keyword - do not remove)
0.0         (deg C)   offset for Tmax
0.0         (deg C)   offset for Tmin
1.0         (DIM)     multiplier for Prcp
1.0         (DIM)     multiplier for VPD
1.0         (DIM)     multiplier for shortwave radiation

CO2_CONTROL   (keyword - do not remove)
1           (flag)    0=constant 1=vary with file 2=constant, file for Ndep
311.17      (ppm)     constant atmospheric CO2 concentration
co2/co2.txt   (file)    annual variable CO2 filename

DISTURBANCE_CONTROL        (keyword - do not remove)
0               (int) number of disturbances

SITE         (keyword) start of site physical constants block
1.0         (m)       effective soil depth (corrected for rock fraction)
56.0         (%)       sand percentage by volume in rock-free soil
38.0         (%)       silt percentage by volume in rock-free soil
6.0         (%)       clay percentage by volume in rock-free soil
2214.0        (m)       site elevation
46.99         (degrees) site latitude (- for S.Hem.)
0.2         (DIM)     site shortwave albedo
0.0001        (kgN/m2/yr) wet+dry atmospheric deposition of N
0.0004        (kgN/m2/yr) symbiotic+asymbiotic fixation of N

RAMP_NDEP     (keyword - do not remove)
0           (flag) do a ramped N-deposition run? 0=no, 1=yes
2099          (int)  reference year for industrial N deposition
0.0001        (kgN/m2/yr) industrial N deposition value

EPC_FILE      (keyword - do not remove)
epc/enf.epc   (file) evergreen needleleaf forest ecophysiological constants

W_STATE       (keyword) start of water state variable initialization block
0.0         (kg/m2)   water stored in snowpack
```

```
0.5         (DIM)     initial soil water as a proportion of saturation

C_STATE      (keyword) start of carbon state variable initialization block
0.001        (kgC/m2)  first-year maximum leaf carbon
0.0          (kgC/m2)  first-year maximum stem carbon
0.0          (kgC/m2)  coarse woody debris carbon
0.0          (kgC/m2)  litter carbon, labile pool
0.0          (kgC/m2)  litter carbon, unshielded cellulose pool
0.0          (kgC/m2)  litter carbon, shielded cellulose pool
0.0          (kgC/m2)  litter carbon, lignin pool
0.0          (kgC/m2)  soil carbon, fast microbial recycling pool
0.0          (kgC/m2)  soil carbon, medium microbial recycling pool
0.0          (kgC/m2)  soil carbon, slow microbial recycling pool
0.0          (kgC/m2)  soil carbon, recalcitrant SOM (slowest)

N_STATE      (keyword) start of nitrogen state variable initialization block
0.0          (kgN/m2)  litter nitrogen, labile pool
0.0          (kgN/m2)  soil nitrogen, mineral pool

OUTPUT_CONTROL   (keyword - do not remove)
outputs/stuartpk_5007     (text) prefix for output files
1   (flag)  1 = write daily output   0 = no daily output
0   (flag)  1 = monthly avg of daily variables  0 = no monthly avg
0   (flag)  1 = annual avg of daily variables   0 = no annual avg
1  (flag)  1 = write annual output  0 = no annual output
1   (flag)  1 = write disturbance text output  0 = no disturbance output
1   (flag)  for on-screen progress indicator

DAILY_OUTPUT     (keyword)
17    (int) number of daily variables to output
0           0 metv.prcp (kg/m2)
1           1 metv.tmax (deg C)
2           2 metv.tmin (deg C)
6           3 metv.tsoil (deg C)
20          4 ws.soilw (kgH2O/m2)
21          5 ws.snoww (kgH2O/m2)
22          6 ws.canopyw (kgH2O/m2)
24          7 ws.outflow_snk (kgH2O/m2)
25          8 ws.soilevap_snk (kgH2O/m2)
26          9 ws.snowsubl_snk (kgH2O/m2)
35          10 wf.prcp_to_canopyw (kgH2O/m2/d)
36          11 wf.prcp_to_soilw (kgH2O/m2/d)
37          12 wf.prcp_to_snow (kgH2O/m2/d)
40          13 wf.snoww_subl (kgH2O/m2/d)
41          14 wf.snoww_to_soilw (kgH2O/m2/d)
42          15 wf.soilw_evap (kgH2O/m2/d)
44          16 wf.soilw_outflow (kgH2O/m2/d)

ANNUAL_OUTPUT    (keyword)
4             (int)   number of annual output variables
21          1 ws.snoww (kgH2O/m2)
26          2 ws.snowsubl_snk (kgH2O/m2)
20          3 ws.soilw (kgH2O/m2)
21          4 ws.snoww (kgH2O/m2)
```

Bibliography

Anderson, E. A. (1976). *A Point Energy and Mass Balance Model of a Snow Cover* (No. NWS 19). Silver Spring, MD: National Weather Service.

Barnett, T. P., Pierce, D. W., Hidalgo, H. G., Bonfils, C., Santer, B. D., Das, T., et al. (2008). Human-Induced Changes in the Hydrology of the Western United States. *Science, 319*(5866), 1080-1083.

Barry, R. G. (1981). *Mountain weather and climate*. New York, NY: Methuen Inc.

Bayard, D., Stahli, M., Parriaux, A., & Fluher, H. (2005). The influence of seasonally frozen soil on the snowmelt runoff at two Alpine sites in southern Switzerland. *Journal of Hydrology, 309*, 66-84.

Bleha, J. A. (2006). *Development and application of a MODIS driven snowmelt model in Northwestern Montana.* University of Montana, Missoula.

Bloschl, G., Kirnbauer, R., & Gutknecht, D. (1991). A spatially distributed snowmelt model for application in alpine terrain. *Snow, Hydrology and Forests in High Alpine Areas*(205), 9.

Briostow, K. L., & Campbell, G. S. (1984). On the Relationship Between Incoming Solar Radiation and Daily Maximum and Minimum Temperature. *Agricultural and Forest Meteorology, 31*(2), 159-166.

Cayan, D. R., Redmond, K. T., & Riddle, L. G. (1999). ENSO and hydrologic extremes in the western United States. *Journal of climate, 12*(9), 2881-2893.

Cline, D. W., Bales, R. C., & Dozier, J. (1998). Estimating the spatial distribution of snow in mountain basins using remote sensing and energy balance modeling. *Water Resources Research, 34*(5), 1275-1285.

Cooley, K. R. (1990). Effects of CO2-induced climate changes on snowpack and streamflow. *Hydrological Sciences Journal, 35*(5), 511-522.

Coughlan, J. C. (1991). *Biophysical aggregation of a forested landscape using a knowledge-based model.* Unpublished Dissertation, University of Montana, Missoula.

Coughlan, J. C., & Running, S. W. (1997). Regional ecosystem simulation: A general model for simulating snow accumulation and melt in mountainous terrain. *Landscape Ecology, 12*(3), 119-136.

Essery, R. (2003). Aggregated and distributed modelling of snow cover for a high-latitude basin. *Global and Planetary Change, 38*(1-2), 115-120.

Ferguson, R. I. (1999). Snowmelt runoff models. *Progress in Physical Geography, 23*(2), 205-227.

Fierz, C., Riber, P., Adams, E. E., Curran, A. R., Fohn, P. M. B., Lehning, M., et al. (2003). Evaluation of snow-surface energy balance models in alpine terrain. *Journal of Hydrology, 282*, 76-94.

Finklin, A. I. (1984). *Weather and Climate of the Selway Bitterroot Wilderness*: Idaho Research Foundation.

Fuchs, T., Rapp, J., Rubel, F., & Rudolf, B. (2000). Correction of Synoptic Precipitation Observations Due to Systematic Measuring Errors with Special Regard to Precipitation Phases. *Physics and Chemistry of the Earth*.

Fuchs, T., Rapp, J., Rubel, F., & Rudolf, B. (2001). Correction of synoptic precipitation observations due to systematic measuring errors with special regard to precipitation phases. *Physics and Chemistry of the Earth 26*(9), 689-693.

Garen, D. C., Johnson, G. J., & Hanson, C. L. (1994). Mean areal precipitation for daily hydrologic modeling in mountainous regions. *Water resources bulletin, 30*, 481-491.

Garen, D. C., & Marks, D. (2005). Spatially distributed energy balance snowmelt modelling in a mountainous river basin: estimation of meteorological inputs and verification of model results. *Journal of Hydrology, 315*(1-4), 126-153.

Geiger, R., Aron, R. H., & Todhunter, P. (2003). *The Climate Near the Ground* (6 ed.). Oxford: Rowman & Littlefield.

Goodison, B. E., Ferguson, H. L., & McKay, G. A. (1981). Measurement and data analysis. In D. M. Gray & D. H. Male (Eds.), *Handbook of Snow* (pp. 191-274). Willowdale, Ontario: Pergamon Press Ltd.

Groisman, P., Peck, E. L., & Quayle, R. G. (1999). Intercomparison of recording and standard nonrecording U.S. gauges. *Journal of atmospheric and oceanic technology, 16*(5), 602-209.

Groisman, P. Y., & Easterling, D. R. (1994). Variability and Trends of Total Precipitation and Snowfall over the United States and Canada. *Journal of Climate, 7*(1), 184-205.

Gustafsson, D., StaÈhli, M., & Jansson, P. E. (2001). The surface energy balance of a snow cover: comparing measurements to two different simulation models. *Theoretical and Applied Climatology, 70*(1-4), 81-96.

Hamlet, A. F., Mote, P. W., Clark, M. P., & Lettenmaier, D. P. (2005). Effects of temperature and precipitation variability on snowpack trends in the western United States. *Journal of Climate, 18*(21), 4545-4561.

Hedstrom, N. R., & Pomeroy, J. W. (1998). Measurements and modelling of snow interception in the boreal forest. *Hydrological Processes, 12*(10-11), 1611-1625.

Hock, R. (2003). Temperature index melt modeling in mountain areas. *Journal of Hydrology, 282*, 104-115.

Hungerford, R. D., Nemani, R. R., Running, S. W., & Coughlan, J. C. (1989). *MTCLIM: A Mountain Microclimate Simulation Model* (No. Research Paper INT-414). Missoula: Intermountain Research Station.

Jordan, R. (1991). *A one-dimensional temperature model for a snow cover*.

Kimball, J. S., Running, S. W., & Nemani, R. (1997). An Improved Method for Estimating Surface Humidity from Daily Minimum Temperature. *Agricultural and Forest Meteorology, 85*, 87-98.

Kimball, J. S., White, M. A., & Running, S. W. (1997). BIOME-BGC simulations of stand hydrologic processes for BOREAS. *Journal of Geophysical Research, 102*(D24), 29,043-029,051.

Kunkel, K. E., & Angel, J. R. (1999). Relationship of ENSO to snowfall and related cyclone activity in the contiguous United States. *Journal of Geophysical Research, 104*(D16), 19,425-419,434.

Kustas, W. P., Rango, A., & Uijlenhoet, R. (1994). A simple energy budget algorithm for the snowmelt runoff model. *Water resources research, 30*(5), 1515-1527.

Lagergren, F., Grelle, A., Lankreijer, H., Molder, M., & Lindroth, A. (2006). Current carbon balance of the forested area in Sweden and its sensitivity to global change as simulated by BIOME-BGC. *Ecosystems, 9*, 894-908.

Lapp, S., Byrne, J., Kienzle, S., & Townshend, I. (2005). Climate Warming Impacts on Snowpack Accumulation in an Alpine Watershed. *International Journal of Climatology, 25*(4), 521-536.

Male, D. H., & Gray, D. M. (1981). Snowcover ablation and runoff. In D. M. Gray & D. H. Male (Eds.), *Handbook of snow: principles, processes, management & use* (1 ed., pp. 360-436). Elmsford, N.Y.: Pergamon Press.

Marks, D., Domingo, J., Susong, D., Link, T., & Garen, D. (1999). A spatially distributed energy balance snowmelt model for application in mountain basins. *Hydrological Processes, 13*(12-13), 1935-1959.

Marks, D., & Dozier, J. (1992). Climate and energy exchange at the snow surface in the alpine region of the sierra nevada 2: snow cover energy balance. *Water Resources Research, 28*(11), 3043-3054.

McCabe, G. J., & Dettinger, M. D. (2002). Primary modes and predictability of year-to-year snowpack variations in the western United States from teleconnections with Pacific Ocean climate. *Journal of Hydrometeorology, 3*(1), 13-26.

Moore, J. N., Harper, J. T., & Greenwood, M. C. (2007). Significance of Trends Toward Earlier Snowmelt Runoff, Columbia and Missouri Basin Headwaters, Western United States. *Geophysical Research Letters, 34*(L16402).

Mote, P. W. (2006). Climate-driven variability and trends in mountain snowpack in western North America. *Journal of Climate, 19*(23), 6209-6220.

Mote, P. W., Hamlet, A. F., Clark, M. P., & Lettenmaier, D. P. (2005). Declining mountain snowpack in western north america. *Bulletin of the American Meteorological Society, 86*, 39-49.

Mote, P. W., Parson, E. A., Hamlet, A. F., Keeton, W. S., Lettenmaier, D., Mantua, N., et al. (2003). Preparing for Climatic Change: The Water, Salmon, and Forests of the Pacific Northwest. *Climatic Change, 61*(1-2), 45-88.

NCDC. (2002). Local Climatological Data, Annual Summary with Comparative Data: Missoula, Montana. In D. o. Commerce (Ed.): National Climatic Data Center, Ashville, NC.

Payne, J. T., Wood, A. W., Hamlet, A. F., Palmer, R. N., & Lettenmaier, D. P. (2004). Mitigating the Effects of Climate Change on the Water Resources of the Columbia River Basin. *Climatic Change, 62*(1-3), 233-256.

Pomeroy, J. W., & Gray, D. M. (1995). *Snowcover accumulation, relocation and management*. Saskatoon, Canada: National Hydrology Research Institute.

Pomeroy, J. W., Parviainen, J., Hedstrom, N., & Gray, D. M. (1998). Coupled modelling of forest snow interception and sublimation. *Hydrological Processes, 12*(15), 2317-2337.

Regonda, S. K., Rajagopalan, B., Clark, M., & Pitlick, J. (2005). Seasonal cycle shifts in hydroclimatology over the western United States. *Journal of Climate, 18*(2), 372-384.

Retzer, J. L. (1974). Alpine soils. In J. D. Ives & R. G. Barry (Eds.), *Arctic and Alpine Environments* (Vol. 1). London: Methuen & Co.

Running, S. W., & Hunt, E. R. (1993). Generalization of a forest ecosystem process model for other biomes, BIOME-BGC, and an application for global-scale models. In J. R. Ehleringer & C. B. Field (Eds.), *Scaling physiological processes: leaf to glove* (pp. 141-158). San Diego: Academic Press.

Running, S. W., & Nemani, R. R. (1991). Regional hydrologic and carbon balance responses of forests resulting from potential climate change. *Climatic Change, 19*(4), 349-368.

Running, S. W., Nemani, R. R., & Hungerford, R. D. (1987). Extrapolation of synoptic meteorological data in mountainous terrain and its use for simulating forest evapotranspiration and photosynthesis. *Canadian journal of forest research, 17*(6), 472-482.

Selkowitz, D. J., Farge, D. B., & Reardon, B. A. (2002). Interannual variation in snowpack in the crown of the continent ecosystem. *Hydrological Processes, 16*(18), 3651-3665.

Semadeni-Davies, A. (1997). Monthly snowmelt modelling for large-scale climate change studies using the degree day approach. *Ecological Modeling, 101*, 303-323.

Serreze, M. C., Clark, M. P., Armstrong, R. L., McGinnis, D. A., & Pulwarty, R. S. (1999). Characteristics of the western United States snowpack from snowpack telemetry (SNOTEL) data. *Water Resources Research, 35*(7), 2145-2160.

Shanley, J. B., & Chalmers, A. (1999). The effect of frozen soil on snowmelt runoff at Sleepers River, Vermont. *Hydrological Processes, 13*, 1843-1857.

Smith, S. R., & O'Brien, J. J. (2000). Regional snowfall distributions associated with ENSO: Implications for seasonal forecasting. *Bulletin of the American Meteorological Society, 82*(6), 11791191.

Spreen, W. C. (1947). A determination of the effect of topography upon precipitation. *Transactions, American Geophysical Union, 28*(2), 285-290.

Stahli, M., & Jansson, P. E. (1998). Test of two SVAT snow submodels during different winter conditions. *Agricultural and Forest Meteorology, 92*(1), 29-41.

Stewart, I. T., Cayan, D. R., & Dettinger, M. D. (2005). Changes toward earlier streamflow timing across western North America. *Journal of Climate, 18*(8), 1136-1155.

Stottlemyer, R., & Troendle, C. A. (2001). Effect of canopy removal on snowpack quantity and quality, Fraser experimental forest, Colorado. *Journal of Hydrology, 245*, 165-176.

Strasser, U., Bernhardt, M., Weber, M., Liston, G. E., & Mauser, W. (2007). Is snow sublimation important in the alpine water balance? *The Cryosphere Discussions, 1*, 303-350.

Susong, D., Marks, D., & Garen, D. (1999). Methods for developing time-series climate surfaces to drive topographically distributed energy- and water-balance models. *Hydrological Processes, 13*(12-13), 2003-2021.

Tague, C. L., & Band, L. E. (2004). RHESSys: Regional Hydro-Ecological Simulation System - An object-oriented approach to spatially distributed modeling of carbon, water, and nutrient cycling. *Earth Interaction, 8*(19), 42.

Taras, B., Sturm, M., & Liston, G. E. (2002). Snow-Ground interface temperatures in teh Kuparuk River Basin, Arctic Alaska: Measurements and model. *Journal of Hydrometeorology, 3*, 377-394.

Tarboton, D. G., & Luce, C. H. (1996). *Utah energy balance snow accumulation and melt model (UEB)*: Utah Water Research Lab and USDA Forest Service Intermounain Research Station.

Thornton, P. E. (1998). *Regional ecosystem simulation: combining surface - and satellite-based observations to study linkages between terrestrial energy and mass budgets.* Unpublished Dissertation, University of Montana, Missoula.

Thornton, P. E., Hasenauer, H., & White, M. A. (2000). Simultaneous Estimation of Daily Solar Radiation and Humidity from Observed Temperature and Precipitation: An Application Over Complex Terrain in Austria. *Agricultural and Forest Meteorology, 104*, 255-271.

Thorton, P. E., & Running, S. W. (1999). An Improved Algorithm for Estimating Incident Daily Solar Radiation from Measurements of Temperature, Humidity, and Precipitation. *Agricultural and Forest Meteorology, 93*, 211-228.

Troendle, C. A., Wilcox, M. S., Bevenger, G. S., & Porth, L. S. (2001). The coon creek water yield augmentation project: implementation of timber harvesting technology on increase streamflow. *Forest Ecology and Management, 143*, 179-187.

Upadhyay, D. S. (1995). *Cold Climate Hydrometeorology* (1 ed.). New York, NY: John Wiley & Sons. Inc.

Viviroli, D., Welngartner, R., & Messerli, B. (2003). Assessing the hydrological significance of the world's mountains. *Mountain Research and Development, 23*(1), 32-40.

Westerstrom, G. (1982). Estimating snow cover runoff by the degree-day approach. *Vannet Norden, 3*, 47-53.

WinSRM. (2003). WinSRM User's Manual. Available at http://hydrolab.arsusda.gov/cgi-bin/srmhome.

Xu, Z. X., Liu, C. M., Ishidaira, H., & Takeuchi, K. (2004). Spatially distributed snowmelt simulation and GIS application in the Wei River basin. *IAHS-AISH Publication, 289*, 114-121.

Yang, D., Goodison, B. E., Metcalfe, J. R., Golubev, V. S., Bates, R., Pangburn, T., et al. (1998). Accuracy of NWS 8" standard nonrecording precipitation gauge: Results and application of WMO intercomparison. *Journal of atmospheric and oceanic technology, 15*(1), 54-68.

Zanotti, F., Endrizzi, S., Bertoldi, G., & Rigon, R. (2004). The GEOTOP snow module. *HYDROLOGICAL PROCESSES, 18*(18), 3667–3679.

Zheng, D., Hunt, E. R., & Running, S. (1993). A Daily Soil Temperature Model Based on Air Temperature and Precipitation for Continental Applications. *Climate Research, 2*, 183-191.